

**Universitat de Lleida**

Document downloaded from:

<http://hdl.handle.net/10459.1/67729>

The final publication is available at:

<https://doi.org/10.1016/j.jhydrol.2013.12.014>

Copyright

cc-by-nc-nd, (c) Elsevier, 2014



Està subjecte a una llicència de [Reconeixement-NoComercial-SenseObraDerivada 4.0 de Creative Commons](https://creativecommons.org/licenses/by-nc-nd/4.0/)

1     **Evaluation of bed load transport formulae in a large regulated**  
2             **gravel bed river: The lower Ebro (NE Iberian Peninsula)**  
3

4                     Raúl López<sup>a, \*</sup>, Damià Vericat<sup>b, c, d</sup>, Ramon J. Batalla<sup>b, c, e</sup>

5  
6     <sup>a</sup> Department of Agricultural and Forest Engineering, University of Lleida, Av.

7     Alcalde Rovira Roure, 191, E-25198, Lleida, Catalonia, Spain, rlopez@eagrof.udl.cat.

8     Tel.+34 973 70 28 20.\* Corresponding author.

9     <sup>b</sup> Department of Environment and Soil Sciences, University of Lleida, Av. Alcalde

10     Rovira Roure, 191, E-25198, Lleida, Catalonia, Spain, dvericat@macs.udl.cat,

11     rbatalla@macs.udl.cat. Permanent address.

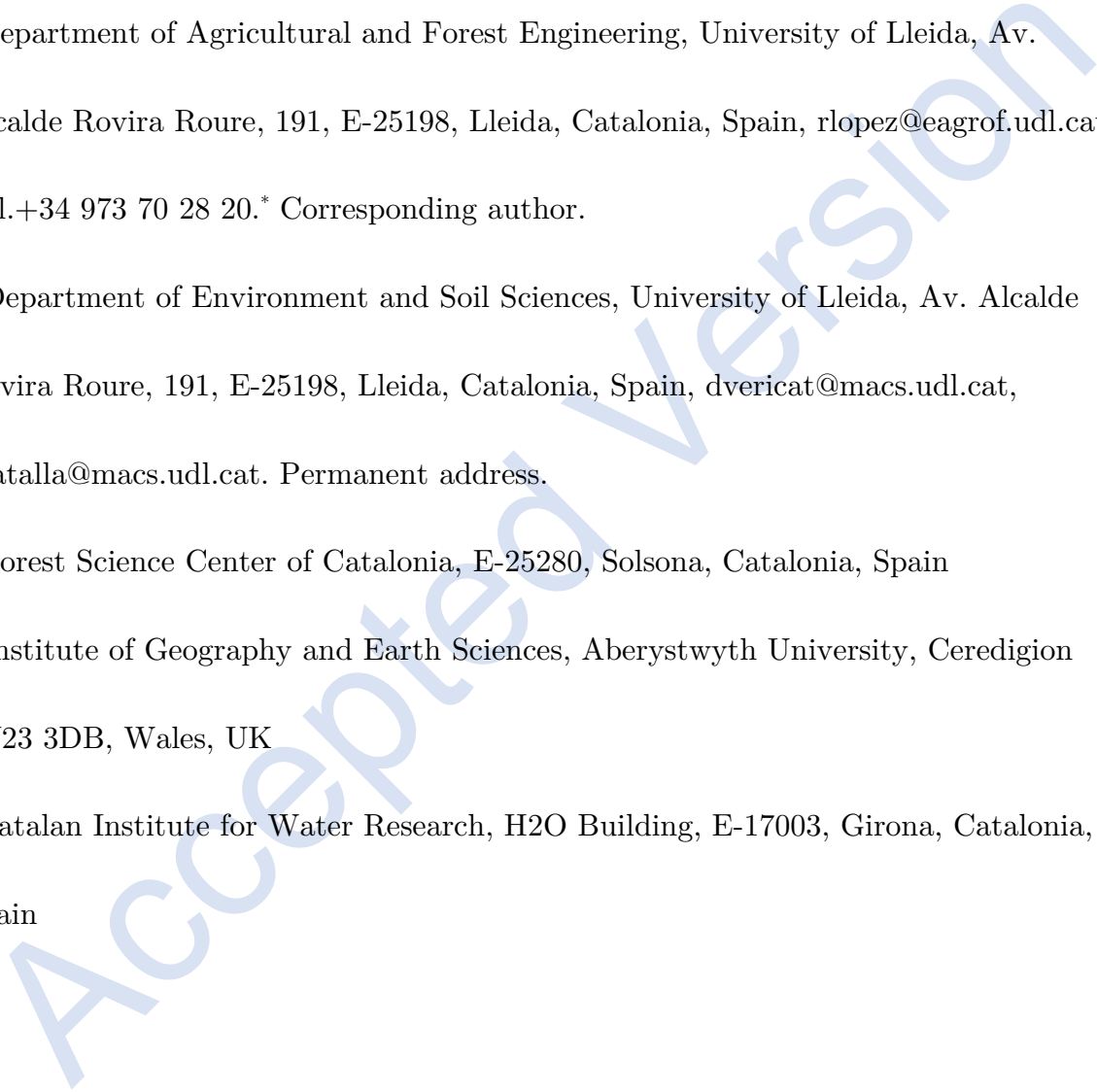
12     <sup>c</sup> Forest Science Center of Catalonia, E-25280, Solsona, Catalonia, Spain

13     <sup>d</sup> Institute of Geography and Earth Sciences, Aberystwyth University, Ceredigion

14     SY23 3DB, Wales, UK

15     <sup>e</sup> Catalan Institute for Water Research, H2O Building, E-17003, Girona, Catalonia,

16     Spain



18 **Abstract**

19

20 This paper tests the predictive power of 10 bed load formulae against bed load rates  
21 obtained for a large regulated river (River Ebro) the armor layer of which is subject  
22 to repeated cycles of break-up and reestablishment. The theoretical principles of two  
23 of the 10 formulae explicitly include the effects of river bed armoring. The results  
24 obtained showed substantial differences in equation performance but no evident  
25 relationship between predictive power and theoretical approach (e.g., discharge,  
26 stream power and probability) was found. Overall, the predictive power of the tested  
27 formulae was relatively low. The average percentages of predicted bed load discharge  
28 that did not exceed factors of 2 ( $0.5 < r < 2$ ) and 10 ( $0.1 < r < 10$ ) in relation to the  
29 observed discharge were 19% and 57%, respectively (where  $r$  is the discrepancy ratio  
30 between the predicted and observed values). In particular, the formulae of Yang  
31 (1984) and Parker et al. (1982) presented the better levels of agreement with the  
32 observed bed load discharges. The bed load rating curve for the lower Ebro showed a  
33 similar degree of agreement to the best-performing formulae. However, its predictive  
34 power was limited because only flow discharge acts as an independent variable and  
35 river bed dynamics, such as armoring cycles, are not contemplated.

36 **Keywords:** Bed load formulae; Bed load transport; Gravel bed-river; Armored bed  
37 river; River Ebro

38

## 39 1. Introduction

40

41 Bed load is the part of the bed material that moves episodically during floods, either  
42 in traction (in rolling or sliding motion), or in saltation in the river channel. It  
43 controls the three-dimensional morphology of rivers and, in consequence, many fluvial  
44 research and management applications require estimates of bed load. Bed load  
45 transport is a highly variable phenomenon, both in space and time. This variability is  
46 reflected in the functional relations that link flow intensity to bed load. Such  
47 relations have an uncertainty that can be placed at some orders of magnitude  
48 (Gomez and Church, 1989). The origin of this lies partly in the highly local and  
49 unsteady nature of the driving forces but is also linked to changing rates of upstream  
50 sediment supply and to the composition and structure of the river bed (Wilcock,  
51 2001; Di Cristo et al., 2006; Greco et al., 2012).

52

53 The main reason for development of bed load equations is the need to predict and  
54 plan in fluvial environments, and not only for engineering purposes. Unfortunately,  
55 the collection of high-quality bed load transport data is an expensive and time-  
56 consuming task, and for many practical purposes recourse is made to a bed load  
57 transport formula (Gómez, 2006). Within this context, numerous bed load transport  
58 formulae have been developed over a century with the main purpose of predicting bed  
59 load, overcoming the inherent variability of sediment transport together with the

60 uncertainties and difficulties associated with sampling. Formulae cover a wide range  
61 of sediment sizes and hydraulic conditions. These formulae are based on the premise  
62 that specific relations exist between hydraulic variables, sedimentary conditions, and  
63 rates of bed load transport (Gomez and Church, 1989). Most of these models have  
64 been derived from flume experimental data (e.g., from early studies such as Gilbert,  
65 1914; Kramer, 1934; Casey, 1935; USWES, 1935; Shields, 1936; Chang, 1939; and  
66 lately Hamamori, 1962) under steady and uniform flow conditions, rather than from  
67 observations of natural flow and transport. Few formulae derive from field  
68 measurements (e.g., Schoklitsch, 1950; Rottner, 1959; Parker et al., 1982; Bathurst,  
69 2007). Inherent bed load transport variability, the changing sedimentary conditions of  
70 the river bed and sampling efficiency are all key components that affect the  
71 performance of equations. Equations are usually calibrated to specific conditions used  
72 to derive them; these may be equilibrium conditions in the case of flume studies, but  
73 this is less likely for equations based on field data.

74  
75 Since the initial comparison made by Johnson (1939) there have been several  
76 assessments of the performance of bed load transport formulae using both field and  
77 laboratory data (e.g., Shulits and Hill, 1968; White et al., 1973; Carson and Griffith,  
78 1987; Yang and Wan, 1991; Chang, 1994; Reid et al., 1996; Batalla, 1997; Martin,  
79 2003; Martin and Ham, 2005). Gomez and Church (1989) undertook one of the most  
80 complete evaluations of bed load formulae and noted that there are more bed load

81 formulae than reliable data to test them (Martin, 2003). These authors concluded  
82 that no formula performs consistently well; this can be attributed to the limitations  
83 of the test data and to the constraints of the test and the physics of the transport  
84 phenomenon. The results of analyses of the performance of these equations have been  
85 published elsewhere. For example, even in the best performing equations evaluated by  
86 White et al. (1975) fewer than 70% of the predicted sediment transport rates lay  
87 between half and twice the observed values. Andrews (1981) showed that the best  
88 equations for predicting bed-material discharges, within a range of half to twice the  
89 observed values, lay between 60% and 79% of the observations. Later, Batalla (1997)  
90 corroborated that the degree of accuracy between observed and predicted values  
91 varies greatly between one formula and another. He reported that the percentage of  
92 observations in which the discrepancy ratio between observed and computed values  
93 had a value of between 0.5 and 2 ranged from 25% (van Rijn) to 38% (Brownlie),  
94 52% (Meyer-Peter and Müller), 65% (Engelund and Hansen), and 68% (Ackers and  
95 White). Most evaluations conclude with a recommendation or representative formula,  
96 but no universal relationship between bed load discharge and hydraulic conditions  
97 has yet been established (Habersack and Laronne, 2002). According to Wilcock  
98 (2001) the lack of field data to test bed load performance and to analyses bed load  
99 transport complexities (e.g., variability) are identified as the key reasons why we  
100 cannot expect to obtain high predictive power of equations under selected conditions.  
101 Testing and verifying formulae in large regulated rivers poses an additional challenge

102 that has not been generally treated in the literature. We specifically refer here to bed  
103 armor condition and its periodic break-up and reformation; these are not exclusive  
104 phenomena of rivers downstream from dams, since many natural gravel-bed rivers  
105 also show this behavior; but regulated rivers may exhibit more extreme conditions of  
106 supply limitation and armor development. In addition, due to channel dimensions  
107 and flow magnitude, large rivers offer less opportunity to obtain direct field data;  
108 field information on such large systems is, in general, sparse and scarce. Finally,  
109 regulated rivers are often subject to management actions, such as the release of  
110 periodical flushing flows that may exacerbate channel adjustments (e.g., Batalla and  
111 Vericat, 2009); those actions should preferably be planned based on empirical data  
112 (in this case bed load and river-bed dynamics) that soundly informs modeling, design,  
113 and implementation and re-evaluation avoiding, this way, completely blind  
114 engineering operations. Within this context, this paper principally aims to assess the  
115 predictive power of a series of bed load formulae tested against bed load transport  
116 rates obtained for a large regulated gravel bed river. Field data were obtained in the  
117 lower River Ebro, downstream from the largest dam complex in the basin, for the  
118 period 2002–2004. This river undergoes cycles of break-up and reestablishment of its  
119 armor layer; this process has been contemplated in the analysis, but for a complete  
120 description, see Vericat and Batalla (2006) and Vericat et al. (2006a). Special  
121 attention has therefore been devoted to studying the performance of formulae under  
122 different armoring conditions; with the objective of informing users of these equations

123 in rivers of similar characteristics where bed load data is unavailable. The novelty of  
124 this investigation relies on the facts that we account for the textural evolution of bed  
125 sediments during the study period, the choice of input grain size (surface vs.  
126 subsurface), and the armoring state. In particular, we show that undertaking analysis  
127 of equation performance as a function of the input grain-size is necessary as an  
128 important factor controlling predicted results. We also present how the observed  
129 scatter in transport rates can be reduced by accounting for textural evolution and  
130 armoring state, which suggests that these factors should be accounted for when  
131 predicting transport rates.

132

## 133 **2. Study Reach and Field Measurements**

134

### 135 **2.1. The lower Ebro**

136

137 The annual runoff of Ebro River basin is highly dependent of mountain regions: the  
138 mountain area only represents about 30% of the total surface area of the Ebro basin  
139 but it is responsible for nearly 60% of its mean annual runoff (López and Justribó,  
140 2010). The Ebro basin is extensively regulated by reservoirs: almost 190 large dams  
141 regulate 67% ( $\approx 7700 \text{ hm}^3$ ) of the river's mean annual runoff. The largest reservoir  
142 complex is located in the lower course of the river and was closed in 1969. It is  
143 comprised by three dams: Mequinenza, Ribarroja and Flix. Together, they impound



144 1750 hm<sup>3</sup> of water (13% of the basin's annual water yield). Frequent floods (i.e.,  $Q_2$ -  
145  $Q_{25}$ , where  $Q_i$  is the discharge associated with an  $i$ -years recurrence interval) have  
146 been reduced by 25% on average (Batalla et al., 2004), while large floods are no  
147 longer observed along this reach.

148

149 Flow hydraulics and sediment transport were regularly and continuously monitored  
150 during floods at the Mora d'Ebre Monitoring Section (hereafter MEMS) during the  
151 period 2002–2004. This section of the river has a channel width of 160 m and is  
152 located 27 km downstream from the Flix Dam. Along this reach, the river flows as a  
153 single, low-sinuosity channel. The mean longitudinal channel slope is  $8.5 \cdot 10^{-4}$ .

154 During the study, the median surface river bed particle size  $D_{50}$  (where  $D$  is the size  
155 of the percentile  $i$  of the grain size distribution) in a gravel bar nearby MEMS ranged  
156 between 33 and 50 mm, while median subsurface size ( $D_{50s}$ ) ranged from 19 to 21  
157 mm. According to these values the mean armoring ratio ranges between 1.6 and 2.6  
158 (armor ratio is estimated as the quotient between the surface and subsurface median  
159 particle size, as per Parker et al., 1982).

160

161 The 2002–2003 and 2003–2004 study periods were average hydrological years in terms  
162 of both the pre-dam and post-dam flow records (Vericat and Batalla, 2006). The  
163 mean discharge was  $415 \text{ m}^3 \cdot \text{s}^{-1}$  for the period 2002–2003 and  $465 \text{ m}^3 \cdot \text{s}^{-1}$  for 2003–  
164 2004. Several floods (some of which were natural and some of which were flushing

165 flows for channel maintenance (see Batalla and Vericat, 2009)) occurred during the  
166 study period and almost all of them were monitored for sediment transport. The  
167 maximum recorded discharge during the study period occurred in February 2003 and  
168 reached  $2500 \text{ m}^3 \cdot \text{s}^{-1}$  (with return period of 8 years, estimated from the post-dam flow  
169 series at the downstream Tortosa gauging station); so we consider this event to be a  
170 large flood in the context of historic flood distribution i.e., largest recorded flood  
171 occurred in 1907 and attained an estimated peak of  $12,000 \text{ m}^3 \cdot \text{s}^{-1}$ . The entire bed  
172 load is trapped in the upstream reservoir complex. As a result, the river does not  
173 receive any coarse-grained bed load fractions from further upstream. However, the  
174 river partially maintains its bed load transport capacity since floods still have enough  
175 competence to entrain river bed sediments downstream from the dam (Vericat and  
176 Batalla, 2006).

177

## 178 **2.2. Field Measurements**

179

180 Here we present a summary of the field methods used to measure discharge, to  
181 characterize river bed sediments and to measure bed load at MEMS. Field  
182 measurements have already been extensively described by Vericat and Batalla (2006)  
183 and Vericat et al. (2006a, 2006b), and further referred in Batalla and Vericat (2009).

184

185 Flow was calculated at the monitoring section by routing hydrographs from an  
186 upstream gauging station operated by the Ebro Water Authorities (Ascó, n. 163, 15  
187 km upstream); and further compared with discharges in Tortosa (n. 27, 49 km  
188 downstream). Discharge measurements were used to corroborate flood hydrographs.  
189 Velocity of the flow was measured from the MEMS bridge by means of an OTT C31  
190 current meter which was attached to a cable-suspended US DH74 sampler. Eleven  
191 velocity profiles were obtained for instantaneous discharges between 750 and  
192  $2160 \text{ m}^3 \cdot \text{s}^{-1}$ . Mean velocities were calculated from velocity profiles and subsequently  
193 used to verify routed discharges from the upstream gauging station.

194  
195 For the purposes of this paper, we used the bed material grain size distribution (i.e.,  
196 surface and subsurface) that was obtained from the closest exposed bar to MEMS.  
197 The bar is located less than 500 m downstream (a distance equivalent to four times  
198 the mean channel width). It is the nearest open and accessible gravel deposit to the  
199 measuring site; we consider it fully representative of the grain-size distribution of the  
200 active sediments in the river (for more details on Ebro's grain size distribution see  
201 Vericat et al., 2006a). Additionally, inactive sediment, which was differentiated by  
202 the vegetation cover, was avoided because it may have little relation with the current  
203 river regime. Bed material sampling was performed on two occasions in relation to  
204 the river's armoring cycle (see methods and results sections for a complete description  
205 and discussion): a) Bed Material I (hereafter BMI) was carried out in summer 2002,

206 i.e., just before the beginning of the 2002-2003 hydrological year; and b) Bed Material  
207 II (hereafter BMII) was undertaken in summer 2003, again just before the beginning  
208 of the 2003-2004 hydrological year. The coarse surface layer was characterized using  
209 the pebble count method (Wolman, 1954; Rice and Church, 1996) in the BMI  
210 characterization. A considerable proportion of fine material (i.e., particles finer than 8  
211 mm) was found at the bed surface in summer 2003 (i.e., BMII characterization); the  
212 surface material was then sampled using the area-by-weight method (Kellerhals and  
213 Bray, 1971). This method offers the possibility of obtaining an accurate  
214 determination of the percentage of fine material as this parameter is known to be  
215 underestimated by the pebble count method. In both campaigns, the surface material  
216 was differentiated from the underlying sediment using spray paint (Lane and Carlson,  
217 1953). The sampled area was then calculated following the Fripp and Diplas (1993)  
218 formula:  $A = 400D_{\max-s}^2$ , where  $A$  is the area ( $\text{m}^2$ ) of the river bed surface that has  
219 to be painted and sampled and  $D_{\max-s}$  is the  $b$ -axis (m) of the exposed particle of  
220 maximum size. Area-by-weight samples were converted to volumetric values  
221 (Kellerhals and Bray, 1971) applying a conversion factor of  $-0.5$  (for more details, see  
222 Vericat et al. (2006a)). The subsurface material was sampled using the volumetric  
223 method after first removing the surface layer. The depth of the subsurface layer was  
224 around 0.3 m; this value lay within the range for the active layer that was observed  
225 during the study period. The largest particle found in the subsurface layer did not  
226 exceed 1% of the sample weight (as per Church et al., 1987). For full coverage of

227 river bed material sampling in the River Ebro, including a discussion about the  
228 precision of measurements and variability in bed material for the whole reach see  
229 Vericat et al. (2006a). Combined bed grain size distributions were generated  
230 according to Fripp and Diplas (1993) and Rice and Haschenburger (2004). Grain size  
231 distributions of the bed material are presented in Figure 1 and Table 1. Figure 1  
232 shows that particles finer than 1 mm are not present in the bed surface, whereas in  
233 the subsurface layer they represent less than 5%, implying that the potential impact  
234 of the sizes transported in suspension on bed load is negligible.

235  
236 Bed load database encompassed 174 samples (124 of which were obtained during the  
237 2002–2003 hydrological year, with the other 50 being obtained in 2003–2004). Around  
238 96% of the total flow range was sampled for bed load during the whole study period.  
239 Bed load was sampled using a cable suspended Helley–Smith sampler with a 152 mm  
240 intake and an expansion ratio of 3.22. Bed load sampling did not exceed 5 minutes  
241 and it was carried out using an automatic crane. Samples were collected in a single  
242 vertical (i.e., channel center). Vericat and Batalla (2005) provided an assessment of  
243 the temporal and spatial variability of bed load transport during steady flow  
244 conditions. Results indicated that bed load sampling at that single vertical  
245 represented exactly the weighted mean bed load of the section in 40% of the samples;  
246 whereas in the other occasions the ratio between cross-sectional rates and bed load at  
247 the vertical ranged from 4 to 6. We consider this sufficient to warrant representation

248 of the total bed load discharge by measurements at the vertical (Vericat and Batalla,  
249 2006).

250

251 As previously mentioned, the  $D_{50}$  of the gravel bar nearby MEMS ranged from 33 to  
252 50 mm, while the largest particles found on the surface measured 117 mm; thus, the  
253 152 mm Helley–Smith should have ensured the efficient sampling of the bed load for  
254 almost all the different grain size classes (for more details on the variability of bed  
255 load and sampling reliability see Vericat and Batalla, 2006, and Vericat et al.,  
256 2006b).

257

### 258 **3. Bed Load Formulae**

259

260 A set of 10 bed load transport formulae were selected. Details of the selected  
261 formulae are presented in Table 2 and fully described in the Appendix A. The main  
262 and most common criterion for selection was that they were commonly applied to  
263 gravel-bedded rivers with moderate to low slope (e.g.,  $< 1\%$ ). Specifically, the  
264 formula that presented an experimental range strictly applicable to the data obtained  
265 for the lower course of the Ebro was the one developed by Bathurst (2007) (hereafter  
266 Bt). Moreover, according to the characteristics of the formulae presented in Table 2,  
267 the size of the bed material in the lower Ebro fits within the experimental range  
268 reported by Bagnold (1980) and Parker et al., (1982) (hereafter referred to as B and

269 P-K-M, respectively). Appendix A presents the formulae as they have been applied in  
270 the present study. Bed load discharge has been calculated in dry weight per unit  
271 width (i.e.,  $q_s$ , where the fundamental dimensions are  $[MT^{-3}]$  expressed in SI units as  
272  $N \cdot s^{-1} \cdot m^{-1}$ ).

273

274 Most of selected formulae in this study were derived from flume experiments, in  
275 which lateral variation of hydraulic variables were not critically important. According  
276 to Ferguson (2003) this type of formulae can lead to underestimate bed load fluxes if  
277 applied to channel where there is a substantial lateral variation in flow hydraulics  
278 (e.g., shear stress). However, in our case study, the river shows a hydraulically wide  
279 channel (i.e., high values of the ratio free surface width/mean flow depth). This  
280 implies that, in practical terms the difference between at-a-section mean values of  
281 hydraulic variables and the values of those variables at the vertical where bed load  
282 was sampled is small. For instance, the mean difference between mean flow depth  
283 and at-a-section and at the sampling vertical was  $\approx 10\%$  (with a maximum value of  
284  $15\%$  during high discharges); whereas the mean difference between at-a-section and  
285 at-a-vertical mean velocity was  $7\%$  (with a maximum value of  $18\%$  during high  
286 discharges). Such flow differences may imply the presence of bedforms, therefore  
287 higher variability in bed load rates could be expected; however, no field evidences are  
288 available to critically analyze this process.

289

290 Some of the selected formulae (e.g., Yang (1984) (hereafter Y) and Parker et al.,  
291 (1982)) explicitly recommended the estimation of fractional bed load rates. This  
292 recommendation was not followed here as we sought to facilitate comparisons  
293 between formulae. For the same reason we also avoid selecting other formulae (e.g.,  
294 Parker, 1990) that require fractional-based bed load transport calculation. Eight of  
295 the chosen formulae specifically estimate bed load transport. The other two, those by  
296 Ackers and White (1973) (hereafter A-W) and Y, permit estimating total bed-  
297 material load. However, in the case of the A-W formula, when the dimensionless  
298 particle diameter exceeds a given threshold, as happens in the Ebro, it is only used to  
299 estimate bed load rates and not bed material transport. In addition, given that the  
300 median diameter of the study reach exceeds the upper application limit of the Y  
301 formulae (i.e., 7 mm) we assume that the gravel concentration in the suspended load  
302 in relation to bed load is negligible in these estimates.

303  
304 A number of theoretical bases for bed load calculation are represented by the selected  
305 formulae. All the main approaches, which include those represented by discharge,  
306 energy slope or shear stress, probability, stream power, regression and equal mobility,  
307 are found in the selected equations (Table 2). The discharge approach adopts critical  
308 water discharge per unit width ( $q_c$ ) as the criterion for determining particle  
309 entrainment and is based on basic field parameters such as sediment size and river  
310 channel slope. The shear stress approach is based on the difference between applied



311 and critical shear stress. The stream power approach relates bed load transport to  
312 power per unit bed area ( $\omega = \rho V y S$ , where  $\omega$  is the stream power per unit bed area  
313 (in mass units),  $\rho$  is the density of the water,  $V$  is the mean flow velocity,  $y$  is the  
314 mean flow depth, and  $S$  is the energy slope) (Bagnold, 1980); or to the power  
315 available per unit weight of fluid ( $\omega' = VS$ , where  $\omega'$  is the stream power per unit  
316 weight of fluid) (Yang, 1973, 1984). In contrast to these deterministic models, the  
317 probabilistic approach relates bed load to fluctuations in the turbulent flow;  
318 furthermore, in the case of the Einstein-Brown (Brown, 1950) formula (hereafter E-B)  
319 no fixed entrainment criterion is defined. The regression approach is typically based  
320 on the statistical fitting of the parameters of an equation obtained by means of  
321 dimensional analysis. Finally, the equal mobility approach assumes that all grain size  
322 ranges are of approximately equal transportability once the critical condition for  
323 breaking the armor has been exceeded.

324

325 Only two of the selected formulae (i.e., P-K-M and Bt) explicitly include in their  
326 theoretical principles the influence of armoring on bed load transport. The other  
327 formulae are based on data that were mostly derived from flume experiments that  
328 did not take into account the effects of armoring on bed load transport. This poses a  
329 serious question relating to selection of the most appropriate river bed particle size  
330 (i.e., surface or subsurface) for the subsequent evaluation of the formulae; the bed

331 material size used to evaluate the formulae selected in this study is extensively  
332 described in section 4.3.

333

## 334 **4. Data Treatment**

335

336 To begin, raw bed load and water discharge data were correlated. Data were  
337 subsequently divided according to periods in which bed-material was sampled (see  
338 next sections 4.1 and 4.2. for a more detailed explanation). Later, in order to create  
339 the database against which the formulae were finally tested, the complete data set  
340 was broken according to two different criteria: bed material characteristics and the  
341 degree of armoring. Data were subsequently grouped by discharge bins; this reduced  
342 the scatter and increased the goodness of the relationship between bed load and  
343 discharge. A detailed explanation of the data treatments is provided in the following  
344 sections and schematically simplified in Table 3.

345

### 346 **4.1. Raw Data**

347

348 A very low degree of correlation was observed between the measured  $q_s$  and  $Q$  in a  
349 log-transformed least-squares best-fit regression (Figure 2a). Often this poor  
350 correlation may be exacerbated by a narrow range of discharge observations. This is  
351 not the case of the Ebro where bed load was sampled from the very onset of motion

352 (at ca.  $600 \text{ m}^3 \cdot \text{s}^{-1}$ ) to flood flows corresponding to a 3-year flood (close to  
353  $1600 \text{ m}^3 \cdot \text{s}^{-1}$ ); under more than fifteen meters of water. In our case, as previously  
354 reported by Vericat et al. (2006a), this variability between  $q_s$  and  $Q$  can be mainly  
355 attributable to the distinct role played by sediment supply-availability and the role of  
356 bed armoring during the study period. The lower Ebro has a well-formed and  
357 dynamic armor layer. This layer is successively broken up and reestablished according  
358 to the magnitude of the flood. The magnitude of the bed load flux increases when the  
359 armor breaks up. This process is always driven by an increment in the supply of  
360 subsurface material to the bed load flux which in turn affects the texture of the  
361 moving material. When the magnitude of subsequent floods is not sufficient to  
362 entrain the whole range of particle sizes on the river bed, the armor reestablishes.  
363 The bed surface then becomes coarser and the bed load becomes more selective.  
364 Under such conditions, at a given discharge, not only can the magnitude of the bed  
365 load flux be very variable, but so too can the texture of the bed load. A full  
366 description of all of these processes is provided in Vericat et al. (2006a).  
367  
368 Table 3 summarizes the different data treatments followed in this study. Bed  
369 material was sampled on two occasions: Bed Material I (BMI in 2002) and Bed  
370 Material II (BMII in 2003) (Table 1). In order to study the influence of bed material  
371 on the relationship between bed load discharge and flow discharge, the complete data  
372 set was partitioned according to the periods in which the different bed materials were

373 sampled. Two sets of bed load samples were therefore derived: a) those collected  
374 between BMI and BMII ( $N = 124$ ); and b) those collected after BMII ( $N = 50$ ). The  
375 bed load samples in a) were called BMI, while those in b) were referred to as BMII  
376 (Table 3). Both groups were plotted against discharge in Figure 2b. The relationships  
377 in this figure show that the BMI bed load samples were the subset of samples that  
378 provided the majority of the scatter in the general relationship presented in Figure  
379 2a. The BMI samples corresponded to a combination of bed load samples that were  
380 obtained under different degrees of armoring (including no armoring).

381

382 The river bed is subject to cyclic incision and armoring processes that are related to  
383 flood magnitude (Vericat et al., 2006a). At the beginning of the study period, the  
384 armor layer was established (i.e., armoring ratio  $\approx 2.6$ ), while during the floods that  
385 occurred between BMI and BMII the armor was broken up as discussed in Vericat et  
386 al. (2006a). We hypothesize that during the process of breaking up the supply of  
387 sediment was highly variable and erratic due to partial disruption of the armor; thus  
388 controlling the high scatter observed for bed load. The pattern observed for the BMII  
389 samples was the more hydraulically driven, presenting less scatter and a clearer  
390 relationship with flow discharge (Figure 2b). The bed material characterization  
391 obtained after the 2002-2003 winter floods that broke up the armor layer (i.e., Bed  
392 Material II in Table 1) indicated that the armoring intensity decreased (i.e., the  
393 armor ratio decreased to 1.6). More relatively fine material was available for the

394 2003-2004 winter floods. These floods were characterized by their relatively low  
395 magnitude compared with those of the previous year. Their competence was not  
396 sufficient to entrain all the bed particle sizes present on the bed; as a result, the  
397 armor layer had become re-established (i.e., mean armoring ratio increased to 2.3) by  
398 the end of the season (Vericat et al., 2006a). Worth to mention, that the mean net  
399 channel incision after high magnitude floods in 2002-2003 was 60 mm. Incision was  
400 minimal during low magnitude floods (i.e.,  $Q_{1-2}$ ) in the following period.

401

402 Taking into account the high variability of the instantaneous bed load rates and the  
403 complex dynamics observed on the river bed (which have been previously described),  
404 we decided to further break or divide the original database ( $N = 174$ ; Table 4),  
405 following two independent criteria: a) the characteristics of the bed material (i.e., Bed  
406 Material Division, BMD) and b) the armor integrity (i.e., Armor Layer Division,  
407 ALD). Once these divisions had been made, the data were independently grouped by  
408 flow discharge class to minimize the degree of scatter and to facilitate comparisons  
409 with bed load formulae predictions (Table 3). More details about the data division  
410 applied can be obtained from Table 4. Note that the main objective of this paper is  
411 not to examine instantaneous bed load variability, but to assess and compare the  
412 predictive power of the selected formulae. The adopted data division is thus fully  
413 justified.

414

## 415 4.2. Data Division

416

417 Bed load data for each division (i.e., BMD and ALD) were grouped following a  
418 discharge class division with range amplitude accounting for approximately 3%  
419 ( $\approx 40 \text{ m}^3 \cdot \text{s}^{-1}$ ) of the total range of measured discharges (from 343 to  $1555 \text{ m}^3 \cdot \text{s}^{-1}$ ).  
420 The scatter of the bed load rates was especially high for discharges of between 343  
421 and  $700 \text{ m}^3 \cdot \text{s}^{-1}$ . Variability may be related to selective transport over the armored  
422 bed. The flow division criterion was therefore not applied to the cited interval and a  
423 single discharge class ( $< 700 \text{ m}^3 \cdot \text{s}^{-1}$ ) was adopted. Overall, as no bed load data were  
424 present for the  $1392\text{-}1433 \text{ m}^3 \cdot \text{s}^{-1}$  class, the total number of discharge bins conforming  
425 the analysis was 21. Class values of  $q_s$  and the rest of the hydraulic variables (mean  
426 depth, mean flow velocity) were obtained as the means of all the values that  
427 constituted each discharge bin or class.

428

### 429 4.2.1. Bed Material Division (BMD)

430

431 By this division, two data sets were obtained: a) all the bed load samples obtained  
432 between BMI and BMII, and b) all the bed load samples collected after BMII (Table  
433 3). All the samples in each set were grouped in accordance with the discharge  
434 approach as outlined above. The result of this treatment was a data set composed of  
435 19 samples for the BMI condition and 17 samples for BMII (Table 4). As previously

436 explained, the number of samples did not reach 21 because no bed load data were  
437 presented for some of the discharge bins. This data set constitutes one of the two  
438 data groupings against which the bed load formulae were tested in this paper.

439

440 Figure 3a shows the relationship between  $q_s$  and  $Q$  for subsets of the BMD. The  
441 degree of correlation of these relations was higher than those obtained for the curves  
442 presented in Figure 2b, the data of which were not grouped by discharge class.

443 However, in absolute terms, the predictive power of the function still remained  
444 limited and well below previously adopted reference values for non-linear i.e., power  
445 relationships (e.g., Barry et al., 2008).

446

#### 447 **4.2.2. Armor Layer Division (ALD)**

448

449 A preliminary analysis of the texture of the bed load samples (Vericat et al., 2006a)  
450 and field observations showed that: i) after the first flood in December 2002, the  
451 armor persisted; ii) the floods registered in February and March 2003 broke up the  
452 armor layer; and iii) the armor was reestablished during the November 2003,  
453 December 2003 and May 2004 flood events. The bed load data set was then divided  
454 in line with these considerations (Table 3). A total of three armor layer conditions  
455 were identified: a) Unbroken Armor Layer (hereafter UAL), b) Broken Armor Layer  
456 (hereafter BAL), and c) Reestablished Armor Layer (hereafter RAL). All of the

457 samples in each division were grouped according to the discharge approach described  
458 above. The result of this treatment was a data set composed of 9 samples for the  
459 UAL condition, and 15 and 17 samples, respectively, for the BAL and RAL  
460 conditions (Table 4). As previously stated, the number of samples did not reach 21  
461 because no bed load data were presented for someone of the discharge bins. It is  
462 necessary to consider that the RAL data subset coincided with the BMII group in the  
463 Bed Material Division; this can be explained by the fact that all of the floods  
464 registered after the BMII bed characterization were classified as events in which the  
465 armor was reestablished. This data set constitutes the second of the two data  
466 groupings against which bed load formulae were tested in this study.

467  
468 Figure 3b shows the relationship between  $q_s$  and  $Q$  as a function of the armor  
469 integrity condition: UAL, BAL, and RAL. This figure shows better grouping and,  
470 certainly, correlations improved when this division was considered; however, for UAL  
471 and BAL the regression coefficients ( $R^2$ ) are still poor. The BAL and UAL relations  
472 are at opposite extremes and clearly represent different sediment supply conditions.  
473 For a given discharge, a larger bed load discharge would be expected for BAL than  
474 for UAL conditions. The RAL condition represents an intermediate position, although  
475 it did not plot very far from the BAL relation (Figure 3b).

476

477



### 478 4.3. Bed Material Input to Formulae

479

480 Transport equations are sensitive to bed-material grain-size, which can differ by a  
481 factor of two or more between surface and subsurface values in armored channels.  
482 Many older bed load equations did not recognize different bed-material domains (i.e.,  
483 surface, subsurface, combined) making unclear which grain-size should be used to  
484 drive transport predictions. Worth to mention that laboratory mixtures used to  
485 derive bed load transport from flume studies can be considered equivalent to the  
486 subsurface sediments typically found in the field, since they distinct input grain-size  
487 that are relevant for equation development and performance. Within this context,  
488 undertaking analysis of equation performance as a function of the input grain-size is  
489 useful, if not necessary, to further highlight its importance as a controlling factor of  
490 predicted results, as we do in this paper. The role of bed load texture (based on bed  
491 load samples) improving formulae prediction was shown by Habersack and Laronne  
492 (2002) emphasizing the sensitivity of model performance to bed material input. In our  
493 study, only 2 of the 10 tested formulae explicitly include in their theoretical  
494 principles the effects of river bed armoring: P-K-M and Bt (Table 2). For the  
495 remaining 8 formulae, different bed material feeding (or input) criteria were adopted  
496 in order to test the role of bed material on bed load predictions. Specifically, the  
497 following considerations were made when selecting the bed texture with which to run  
498 the analysis:

499

500

1. Bed Material Division (BMI and BMII data sets): (A) a first run of the formulae was conducted using the subsurface grain size distribution from the samples obtained in 2002 (i.e., BMI) and 2003 (i.e., BMII, see Table 1 for more details). A total of 36 predictions were obtained. (B) The formulae were subsequently run using the surface grain size distributions obtained for each period (i.e., BMI and BMII). As in the consideration (A), a total of 36 predictions were calculated.

507

508

2. Armor Layer Division (UAL, BAL and RAL data sets): in this case the texture inputs of the formulae were related to the armor condition for each data set. (A) Unbroken Armor Layer (UAL): the formulae were run using the surface grain size distribution obtained in BMI; (B) Broken Armor Layer (BAL): a combined grain size distribution for the BMI period was used.

513

Surface and subsurface materials were combined in a single grain size

514

distribution as described in Section 2.2 and can be seen in Figure 1b; and,

515

finally (C) Reestablished Armor Layer (RAL): the surface grain size

516

distribution obtained during BMII was used as input for the formula texture.

517

A total of 41 predictions were obtained (Table 4). It is worth mentioning that

518

analysis based on the Armor Layer Division may provide a better

519

understanding of the observed phenomena with greater explanatory power

520 since it allows a more accurate adjustment of the grain size distribution in line  
521 with the particular conditions of each of the flood events analyzed.

522

523 The texture input in the P-K-M and Bt formulae, which explicitly include the effects  
524 of river bed armoring in their respective theoretical principles, requires further  
525 consideration. In both of these cases, the formula in question directly specify the  
526 (surface or subsurface) material required to predict bed load discharge i.e., P-K-M  
527 (only subsurface) and Bt (surface and subsurface). Moreover, these formulae can only  
528 be applied once the armor has been broken, a condition that is estimated by the  
529 formulae. These formulae will therefore only be applied for: a) samples in BMI and  
530 BMII (Bed Material Division) that exceed the armor breaking condition estimated by  
531 the formulae, and b) samples in BAL (Armor Layer Division) if the formulae predict  
532 that the armor will be broken.

533

534 It is widely acknowledge that textural evolution of the bed affects transport rates  
535 during and between floods (e.g., Parker and Klingeman, 1982; Dietrich et al., 1989;  
536 Parker, 1990; Vericat et al., 2006a; Turowski et al., 2011). However, few studies  
537 account for this variability when applying bed load transport equations and none  
538 examine such effects on equation performance. Although at a different temporal scale  
539 (i.e., annual instead of flood), our approach takes into account the variability of bed  
540 characteristics and its influence on formulae performance, by considering an Armor

541 Layer Division: unbroken, broken and reestablishment conditions; a fact that reflects  
542 the progressive changes in bed surface grain-size.

543

## 544 **5. Assessment of Formulae Performance**

545

546 The predictive power of selected formulae was assessed and ranked by comparing  
547 observed ( $q_{so}$ ) and predicted ( $q_{sp}$ ) values of the unit bed load discharge. The main  
548 issues assessing formulae performance relate to (a) formulae that erroneously predict  
549 zero bed load transport, and (b) to the deviation between  $q_{so}$  and  $q_{sp}$  that typically  
550 span a large range of values (both in absolute ( $q_{so}-q_{sp}$ ) and relative ( $q_{so}/q_{sp}$ ) terms).

551

552 These issues were addressed in the following way. Incorrect zero predictions (i.e.,  $q_{sp}$   
553 = 0) may be obtained at low flow rates if the averaged predicted threshold value for  
554 particle entrainment is not exceeded. Zero bed load predictions are incompatible with  
555 many of the statistical indices commonly used to assess formulae performance. One  
556 frequent solution is the substitution of zero predictions by a minimum value of bed  
557 load discharge (e.g., Barry et al., 2004, 2007; Recking, 2010). Occasionally, if the  
558 proportion of zero predictions is significant, some indices may end up as functions of  
559 the minimum adopted values of  $q_{sp}$  rather than as real indicators of formula  
560 performance (e.g., Barry et al., 2007). In this study, we took a minimum value of  $q_{sp}$   
561 ( $m q_{sp}$ ) adapted to the minimum observed value of  $q_{so}$  for each of the data subgroups

562 (BMD and ALD), but based on a sensitivity analysis undertaken for the different  
563 statistical indices. We examined the effect of a wide variation of  $mq_{sp}$  (i.e., between  
564  $10^{-9}$  and  $10^{-2} \text{ N}\cdot\text{s}^{-1}\cdot\text{m}^{-1}$ ) for all the statistical indices. Although these indices are  
565 properly introduced further in the text, this analysis illustrated as equations showed  
566 progressively better adjustment with the increase of the  $mq_{sp}$  value adopted for  
567 predictions 0. It is worth to mention, the selected value of  $mq_{sp}$  only begins to affect  
568 the arithmetic mean of the discrepancy ratio (i.e.,  $mr$ , index further introduced) for  
569 almost all the equations when  $mq_{sp}$  was greater than a given value; a value that was  
570 adopted for selecting  $mq_{sp}$  for each data division. Specifically, in the case of the Bed  
571 Material Division database the critical value of  $mq_{sp}$  was around  $10^{-3} \text{ N}\cdot\text{s}^{-1}\cdot\text{m}^{-1}$ ,  
572 representing the 65% of the minimum  $q_{so}$ , which was exceeded by 93% of the values  
573 in the original dataset ( $N = 174$ ). In the case of the Armor Layer Division database,  
574 however, the critical value of  $mq_{sp}$  was around  $4 \cdot 10^{-5} \text{ N}\cdot\text{s}^{-1}\cdot\text{m}^{-1}$ , a value that  
575 represented 62% of the minimum  $q_{so}$ , which was exceeded by 99% of the values in the  
576 original dataset.

577

578 Several statistical indices and graphical methods were used to assess the performance  
579 of the different formulae. These indices are based on the discrepancy ratio ( $r$ )  
580 between the predicted and observed values ( $r = q_{sp}/q_{so}$ ). The range of this ratio  
581 is  $(0, +\infty)$ . In bed load studies  $r$  can span a large range of values: frequently two or  
582 more orders of magnitude (e.g., Duan et al., 2006; Recking, 2010). Statistical

583 comparisons should therefore also include log transformations and indices that are  
584 less sensitive to extreme values.

585

586 First, we calculated the percentage of  $q_{sp}$  that did not exceed a factor of 2 ( $0.5 < r <$   
587  $2$ ), 5 ( $0.5 < r < 2$ ) and 10 ( $0.1 < r < 10$ ) in relation to  $q_{so}$ . The arithmetic mean of  $r$   
588 ( $mr$ ) was also used:

589

$$mr = \frac{1}{N} \sum_{i=1}^N r_i \quad (1)$$

590

591 where  $r_i$  is the  $i$  value of  $r$ , and  $N$  is the number of data. This value is in the  
592 range  $(0, +\infty)$ , with values close to 1 indicating less discrepancy. The arithmetic  
593 mean of  $\log r$  ( $mlr$ ) was also used:

594

$$mlr = \frac{1}{N} \sum_{i=1}^N \log r_i \quad (2)$$

595

596 where  $r_i$  is the  $i^{\text{th}}$  value of  $r$ , and  $N$  is the number of data. This value is in the  
597 range  $(-\infty, +\infty)$ , with values close to 0 indicating less discrepancy. A modified type  
598 of geometric mean value of  $r$  ( $gr$ ) (Habersack and Laronne, 2002) was also used:

599

$$gr = (r_1 r_2 \cdots r_i \cdots r_N)^{1/N} \quad (3)$$

601

602 where the reciprocal value is used if  $r_i < 1$ , ensuring that  $gr \geq 1$ . This value is in the  
603 range  $(1, +\infty)$ , with low values indicating the smallest discrepancies. A weighted  
604 variation of the  $gr$  index ( $gwr$ ) (Habersack and Laronne, 2002) was also used:

605

$$606 \quad gwr = (rw_1 rw_2 \cdots rw_i \cdots rw_N)^{1/N} \quad (4)$$

607

608 where  $rw$  is a value of  $r$  weighted by the power of the observed bed load discharge  
609 ( $rw = r^{q_{so}}$ ) and where the reciprocal value is used if  $rw_i < 1$ , ensuring that  $gwr \geq 1$ .

610 This value is in the range  $(1, +\infty)$ , with low values indicating the smallest  
611 discrepancies between  $q_{sp}$  and  $q_{so}$ .

612

613 We also graphically examined (at the log scale) the deviation between  $q_{so}$  and  $q_{sp}$  for  
614 each bed load transport value and we analyzed the distribution of the discrepancy  
615 ratio ( $r$ ) using a box-plot diagram at the logarithmic scale. The ranking of the  
616 performances of different formulae may vary according to the statistical properties of  
617 the indices in question (e.g., Habersack and Laronne, 2002; Barry et al., 2007). For  
618 instance, the  $mr$  index is more sensitive to  $r$  values larger than 1 (i.e., a value of  $r =$   
619 10 weighs more in the  $mr$  computation than a value of 0.1, despite the fact that both  
620 represent a deviation of one order of magnitude with respect to the symmetry axes  $r$   
621  $= 1$ ). The  $mr$  index is therefore less sensitive to the proportion of zero predictions

622 and also to the minimum adopted value of  $q_{sp}$ . In contrast, in the  $mrl$  index, errors of  
623 equal magnitude weigh the same, independently of their relative positions with  
624 respect to the symmetry axes  $\log r = 0$  (e.g.,  $r = 10$  and  $r = 0.1$ ). It is therefore more  
625 sensitive to the proportion of zero predictions and to the minimum adopted value of  
626  $q_{sp}$ . A limitation of  $mrl$  is that  $\log r$  values of the same magnitude and opposite signs  
627 cancel each other out, yielding  $mrl = 0$ . This index is therefore more sensitive to  
628 small but asymmetrical deviations (e.g., if  $r_1 = 1.5$  and  $r_2 = 2$  then  $mrl = 0.24$ ) than  
629 to larger symmetrical deviations (e.g., if  $r_1 = 0.01$  and  $r_2 = 100$  then  $mrl = 0$ ).  
630 Furthermore,  $gr$  is less sensitive than  $mr$  to high values of  $r$  (i.e.,  $r \gg 1$ ) because it  
631 is based on the geometric mean; however, it is more sensitive to zero predictions,  
632 since a reciprocal value is taken if  $r < 1$ . Finally, the  $gwr$  index is more sensitive to  
633 deviations of large  $q_{so}$  values. Previous works (e.g., Barry et al., 2007) conclude that,  
634 given the potential bias of error index, there is no perfect method for assessing  
635 equation performance, especially in those cases that allows for inclusion of incorrect  
636 zero predictions.  
637  
638 The performance of the formulae is ranked for each index. The global performance of  
639 the formulae is assessed on the basis of a combination of three different criteria: a)  
640 the relative position for each index, b) the frequency with which the formulae are  
641 located in the top five positions, and c) the ratio between the index value obtained  
642 using a given formula and the lowest index value (i.e., this last value is determined



643 by the lowest ranked formula). We also present the log scale comparison between  $q_{sp}$   
644 and  $q_{so}$  for the Bed Material and Armor Layer divisions. Finally, we present a box  
645 plot in log scale corresponding to the distribution of the discrepancy ratio ( $r$ ) for: a)  
646 BMD (fed with subsurface bed material), b) BMD (fed with surface bed material),  
647 and c) ALD divisions.

648

## 649 **6. Bed Load Regime**

650

651 A full description of the flow and bed load regime during the period 2002–2004 was  
652 reported by Vericat and Batalla (2006); hence, only a brief summary is presented  
653 here to contextualize the main results of this paper. Bed load was sampled during  
654 almost all of the floods recorded during that period. The mean bed load rate was 1.36  
655  $\text{N} \cdot \text{s}^{-1} \cdot \text{m}^{-1}$  in 2002–2003 (i.e., BMI) and  $0.65 \cdot 10^{-1} \text{N} \cdot \text{s}^{-1} \cdot \text{m}^{-1}$  in 2003–2004 (i.e.,  
656 BMII). Worth to notice that that bed load rates during the first period show a highly  
657 variable pattern for a given discharge (Figure 2b), contributing to a high scatter in  
658 the plot. Maximum rates were recorded in 2002–2003, with an instantaneous  
659 maximum value of  $11.8 \text{N} \cdot \text{s}^{-1} \cdot \text{m}^{-1}$  (for further details, see Vericat and Batalla  
660 (2006)).

661

662 Bed load texture was markedly different in the two periods. The median bed load  
663 particle size in the samples collected during the period 2002–2003 varied from 1 to 72

664 mm, while for 2003–2004 this range decreased to 4–44 mm, showing a more selective  
665 transport range. The upper limits of both ranges corresponded to the  $D_{70}$  and  $D_{65}$  of  
666 the bed surface grain size distribution obtained in 2002 and 2003 respectively (Figure  
667 1). The lower limit was not present in the surface sediments sampled in 2002 and  
668 represents the  $D_{15}$  of the 2003 distribution.

669  
670 The original database ( $N = 174$ ) was grouped according to the previously reported  
671 discharge class division in order to define a bed load rating curve for the lower Ebro.  
672 Note that in this case data were not divided according to any specific bed material or  
673 armor integrity criteria. The corresponding bed load transport model is:

$$674 \quad q_s = 4 \cdot 10^{-10} Q^{3.11} \quad (5)$$

675  
676  
677 ( $R^2 = 0.46$ ,  $N = 21$ ,  $p = 7.3 \cdot 10^{-4}$ ). The statistical indices applied for the formulae  
678 were also obtained for Eq. (5). Note that this equation is not comparable with the  
679 rest of assessed formulae, since it is a regression equation derived from own data of  
680 the study reach. Although indices for Eq. (5) were not taken into account in the  
681 ranking of the formulae, they are shown at the bottom of the tables 5, 6 and 7 in  
682 order to facilitate comparisons between the Ebro bed load model and the 10 different  
683 formulae that were selected.

## 684 7. Testing the Formulae

685

### 686 7.1. Bed Material Division

687

688 Tables 5 and 6 show the statistical indices according to the Bed Material Division  
689 and considering the different sediment grain-size scenarios (i.e., subsurface and  
690 surface, respectively). In these tables, the value of each statistical index is ordered  
691 from the smallest to the largest discrepancy between the values for  $q_{sp}$  and  $q_{so}$ ; this is  
692 a way of ranking the predictive power of each formula. It is important to note that  
693 we have included formulae that explicitly consider the presence of an armor layer  
694 (i.e., P-K-M and Bt) (Tables 5 and 6) despite these formulae directly specify the  
695 material (i.e., surface and/or subsurface) required to predict bed load discharge (see  
696 section 4.3).

697

698 When we used subsurface grain size distribution in the BMD the overall best fit was  
699 provided by P-K-M, B, Y and the Rottner (1959) (hereafter R) formulae (Table 5).

700 This can be seen in Figures 4 and 6a in which these three formulae show less scatter

701 than the others. The worst performing formulae were those of Meyer-Peter and

702 Müller (1948) (hereafter M-P-M), E-B and Wong and Parker (2006) (hereafter W-P);

703 mainly due to their trend to overpredict. When the surface bed material was used in

704 the BMD, there were smaller discrepancies between P-K-M and Y and the observed

705 data (Table 6). However, Figure 6b reveals that Y produced greater scatter for  $r$   
706 than P-K-M (especially for the lower limit, since the Y formula predicted no bed load  
707 discharge (i.e., zero bed load) for 5 values (see Figure 4)). The E-B formula  
708 performed well, although it showed a larger scatter of  $r$  between percentiles 25 and 75  
709 (Figure 6b). The worst performing formulae were B and S, mainly because they  
710 tended to underestimation (Figures 4 and 6b).

711

712 Figures 4, 6a and 6b illustrate an overall tendency to underestimate (e.g., median  
713 discrepancy ratio  $r < 1$ ) when surface material is used; in contrast, overestimation  
714 occurs when subsurface material is used as a grain-size predictive variable (e.g.,  
715 median discrepancy ratio  $r > 1$ ). All the formulae (except P-K-M and Bt) that use  
716 subsurface material yielded an arithmetic mean of the median values of  $r$  (where the  
717 reciprocal value was used if the median value of  $r < 1$ ) of 9.3, with a coefficient of  
718 variation of 125%. When surface material was used, the arithmetic mean of the  
719 median values of  $r$  (where the reciprocal value was used if the median value of  $r < 1$ )  
720 was 112 and the coefficient of variation was 126%. Underestimation using surface  
721 material is therefore, on average, one order of magnitude higher than overestimation  
722 using subsurface material. This pattern can mainly be attributed to the fact that  
723 surface material was too coarse to be theoretically entrained for most of the eight  
724 formulae. In similar way, the relative fine texture of the subsurface materials drives

725 to overprediction. Figure 4 illustrates the different proportion of zero bed load  
726 predictions when using surface and subsurface materials.

727

728 Finally, armoring was greater for BMI than for BMII (Table 1). This may explain the  
729 larger discrepancy between the predictions when surface and subsurface materials  
730 were alternatively used to feed the formulae under the BMI division (Figure 4). In  
731 some cases this discrepancy was notably large since the surface material for BMI was  
732 too coarse for the flow to exceed the predicted entrainment threshold (which was  
733 based on the formulation, see Appendix A). This was evident, especially for equations  
734 S, B, W-P and A-W; none of these equations showed more than three values (for  
735 BMI surface material) that exceeded the entrainment condition value (Figure 4).

736

## 737 **7.2. Armor Layer Division**

738

739 Table 7 shows the values of indices according to the Armor Layer Division. In this  
740 table, each of the statistical index values is ordered from small to large discrepancies  
741 between  $q_{sp}$  and  $q_{so}$ ; this makes it possible to rank the predictive power of each  
742 formula.

743

744 P-K-M and Y show the best performance, followed by the W-P formula (Table 7).

745 Figure 6c shows that the P-K-M formula produced much less scatter than the other

746 two equations. This may be due to the fact that P-K-M predictions only  
747 corresponded to data from the Broken Armor Layer (BAL) subgroup (see section  
748 4.3.); whereas predictions by the other two formulae experienced the negative impact  
749 of zero predictions in the Unbroken Armor Layer (UAL) subgroup (Figure 5). Bt, B  
750 and A-W showed the lowest levels of predictive power.

751

752 Figure 3b illustrates that the bed load rating curve for the BAL data subgroup  
753 plotted above the curves of the UAL and Reestablished Armor Layer (RAL), with  
754 higher values of  $q_s$  for the same value of  $Q$ , showing the effects of the armor break-up.  
755 BAL and RAL are the two closest subgroups in Figure 3b, with an overlap for  $q_s$   
756 between  $0.5$  and  $1.50 \text{ N} \cdot \text{s}^{-1} \cdot \text{m}^{-1}$ . In contrast to RAL, there are up to seven values of  
757 BAL for  $q_s > 1.50 \text{ N} \cdot \text{s}^{-1} \cdot \text{m}^{-1}$ . However, this trend was not well predicted by most of  
758 the formulae that were studied. Figure 5 indicates that frequently predicted  $q_s$  values  
759 for RAL plotted at the same level, or even higher level, than those of the BAL  
760 subgroup. This can mainly be attributed to the fact that the combined bed material  
761 of BMI applied for BAL condition is similar to the surface material of BMII (used  
762 under RAL conditions). In contrast, most of the predictions for the UAL subgroup  
763 were below those obtained for BAL and RAL (Figure 5); most of the predictions for  
764 UAL yielded 0 (except for the E-B and Y formulae). This may have been related to  
765 the coarse size of the BMI surface bed-material (Table 1).

766

767 Overall, a larger deviation between predicted and measured bed load discharge was  
768 observed for low flow discharges near the observed threshold of mobility (e.g.,  
769 Habersack and Laronne, 2002; Barry et al., 2004; Recking, 2010). This would be the  
770 case of the predictions from E-B and Y in relation to the lowest observed values for  
771 the UAL subgroup (Figure 5). The fact that the UAL data were the ones with the  
772 largest proportion of  $q_{so} < 0.01 \text{ N}\cdot\text{s}^{-1} \cdot \text{m}^{-1}$  (Figure 3b) helps to explain the poor  
773 performance of the formulae tested for this subgroup. This also explains why the  
774 global performances of most of the formulae were not appreciably better for the  
775 Armor Layer Division than for the Bed Material Division (fed by subsurface  
776 material). However, for the ALD condition and all the formulae, the arithmetic mean  
777 of the median values of  $r$  (where the reciprocal value was used if the median value of  
778  $r < 1$ ) was 7.4 and the coefficient of variation was 88% (7.6 and 91%, respectively, if  
779 P-K-M and Bt are excluded). These are more significant values than the obtained for  
780 the BMD condition (see section 7.1). This fact indicates, in general terms, that  
781 considering the armor condition improves the explanatory power of the bed load  
782 formulae.

783

## 784 **8. Discussion**

785

786 The results show that the predictive power of the tested formulae is relatively low,  
787 although on the range observed in the literature. The low accuracy of the formulae is

788 known by every engineering standard, where commonly a much higher accuracy is  
789 required. Overall, including the 10 formulae and all the scenario divisions, the  
790 average percentages of predicted bed load discharge ( $q_{sp}$ ) not exceeding a factor of 2  
791 ( $0.5 < r < 2$ ), 5 ( $0.2 < r < 5$ ) and 10 ( $0.1 < r < 10$ ) in relation to the observed  
792 discharge ( $q_{so}$ ) were 19%, 41% and 57%, respectively. Although this degree of  
793 discrepancy may seem rather large, it is not unreasonable in comparison to previous  
794 studies that explored the performance of bed load transport formulae in gravel  
795 bedded rivers (see Table 8 for comparison with a selection of recent studies). Worth  
796 to point out that our results and consequent conclusions may be sensitive to the  
797 available sampling period (2 years) and the small sample size (one river). A longer  
798 sampling period might weight the distribution of observed transport rates differently  
799 than those observed over the current 2-year period, potentially changing equation  
800 performance. However, the advantage of the sampled years is that these represent  
801 significantly different bed conditions; more stable because the well-developed armor  
802 layer and more mobile because the effects of the break-up of the armor layer. These  
803 conditions are also sensitive to bed load performance as is analyzed in this study.  
804 Equation performance also varies between rivers (e.g., Barry et al., 2008) and that  
805 results might differ if the analyses had been conducted across a range of rivers.  
806  
807 The P-K-M (Parker et al., 1982) and Y (Yang, 1984) formulae presented the better  
808 levels of agreement with observed bed load discharges. Overall, these formulae were



809 always ranked in the first positions according to the combined evaluation criteria.

810 The Y formula maintained a high predictive power (i.e., relatively good performance)

811 even when the bed texture used for its formulation changed from subsurface to

812 surface material (in the Bed Material Division, BMD). This is related to the

813 relatively low sensitivity of the formula to the bed material in question, which is

814 discussed later in this section. The P-K-M formula, in contrast, does not take into

815 account the bed material criteria; the formula is run when it is considered that the

816 driving force exceeds the armor break up condition. The performance of the majority

817 of the formulae declined when surface material is used in the BMD. Also was

818 observed the variability in ranking of formulae performance once the bed texture had

819 changed. For instance, B formulae (Bagnold, 1980), E-B (Einstein-Brown, in Brown,

820 1950), W-P (Wong and Parker, 2006) appear either near the top or near the bottom

821 of the performance ranking depending on the bed texture used in their calculations.

822

823 In global terms, although the results show substantial differences in equation

824 performance, no evident and categorical relationships were found between the

825 predictive power of the formulae and their theoretical approach. However, in this

826 study, the formulae that performed best maintained their accuracy much more

827 constantly over the whole range of discharges than formulae with a low level of

828 performance and whose accuracy was highly variable. This pattern is observed in

829 Figure 4 by comparing the performance of the P-K-M, B and Y formulae with those

830 of the E-B and MP-M formulae. More specifically, the latter group shows how  
831 overestimation increases as bed load discharge decreases. Equation performance may  
832 vary in relation to site characteristics, sampling conditions and representativeness.  
833 For instance, Barry et al., (2008) attributed part of this discrepancy to differences in  
834 the frequency of the discharges used for assessing the performance of these equations  
835 (e.g., bankfull discharge vs. low flows).

836

837 Only 2 of the 10 formulae that were tested explicitly include the effects of river bed  
838 armoring in their theoretical principles: P-K-M and Bt (see Appendix A and Table  
839 2). The Bt formula only quantifies bed load discharge once the armor has been  
840 broken, while the P-K-M formula considers equal mobility once the armor has been  
841 broken (see Appendix A for criteria). As a result, only the predictions that exceeded  
842 the threshold above which the armor layer broke were considered when these two  
843 formulae were evaluated according to the Bed Material Division. In turn, only the  
844 predictions within the Break Armor Layer (BAL) group were considered when these  
845 formulae were evaluated according to the Armor Layer Division. Taking these  
846 considerations into account, the discrepancy between predicted and observed bed  
847 load discharges was smaller in the case of the P-K-M formula than in that of Bt  
848 (Figure 6). P-K-M formula that presented one of the best levels of agreement with  
849 the observed bed load discharges, as discussed above. In contrast, the Bt formula was  
850 ranked within the five worst formulae in terms of prediction. In this case, the

851 relatively poor performance could be attributed to the overestimation of the threshold  
852 above which the armor layer breaks up.

853

854 As already pointed out, the Yang formula produced one of the best performances,  
855 irrespective of the division that was considered. However, it is worth noting that in  
856 some cases the Y formula predicts an increase in bed load rates associated with an  
857 increase in sediment grain size (see Figures 4 and 5); this observation contradicts the  
858 physical phenomena that were modeled. A similar finding was reported by Chang  
859 (1988) and Julien (1998); for the sand bed load formula by the same author (i.e.,  
860 Yang, 1973) a slight increase in sediment transport capacity was detected with grain  
861 size for coarse sands. The Y formula is not as sensitive to grain-size as other  
862 formulae, and, therefore, is less likely to produce wide variations in calculated  
863 sediment transport (USACE, 1989). Similarly, the Y formula performed consistently  
864 well even when surface material was substituted by subsurface material in the BMD  
865 analysis; this contrasted with the observed decrease in predictive power shown by  
866 most of the other equations that were studied.

867

868 The overestimation by the MP-M formula observed in this study could have been due  
869 to the adoption of the plane-bed hypothesis (i.e.,  $k/k' = 1$  and therefore no form of  
870 drag correction); although several studies have already detected that it overpredicts  
871 bed load transport under plane-bed conditions (i.e., in the absence of a form drag

872 correction) (Wong and Parker, 2006). It should be noted that the W-P formula was  
873 developed as an improved version of the MP-M equation using part of the original  
874 database (Table 2). The results obtained show significantly smaller estimates than  
875 those produced by the original formula under plane-bed conditions (with differences  
876 of a factor of 2.0-2.5) (Wong and Parker, 2006). Our results indicate that the MP-M  
877 formula (with no form drag correction) predicts higher rates than those obtained by  
878 the W-P equation; the values differed by a factor of between 2 and 3 once the  
879 entrainment threshold had been exceeded.

880  
881 The best predictions of the Ebro bed load rating curve (Eq. (5)) were similar to those  
882 of the best performing formulae. The best predictions were obtained for the BMD  
883 using surface material; in this case, our model produced the best performance  
884 according to five of the seven statistical indices (Table 6). In contrast, its  
885 performance for ALD analysis was not significantly better than that of the other 10  
886 equations (Table 7). This may be attributed to the large discrepancy associated with  
887 the Unbroken Armor Layer condition (see Figure 3b). Although the regression  
888 expressed in Eq. (5) was statistically significant, it only explained 46% of the bed  
889 load variability. Overall, we can conclude that the performance of Eq. (5) was not  
890 definitely better than the best ranked models analyzed in this study. In the case of  
891 the Ebro, the predictive power of the general bed load model was clearly limited  
892 because the only independent variable was flow discharge; as a result, the equation

893 cannot fully explain phenomena such as the temporal variability of bed grain-size or  
894 the cycle according to which armor layer was broken up and re-established during the  
895 study period.

896

897 Our work principally aimed at assessing the predictive power of a series of bed load  
898 formulae tested against bed load transport rates obtained for a large regulated gravel  
899 bed river. We do not intend at any kind of formulae calibration or process-based  
900 reassessment; but to give practitioners a guide of formulae performance applicable to  
901 large regulated rivers in which, generally, field data is scarce and riverbed dynamics  
902 difficult to observe. Results provide insights into variability of real processes and  
903 model performance, according to bed material characteristics and structure (Figure  
904 7). Although, on average, bed surface material provides best model performance, it is  
905 worth to notice that models predicting the lowest transport rates (lower envelopes in  
906 figure 7) best resembles the observed Ebro model (Eq. (5)), when they are fed with  
907 subsurface material (Figure 7a). This fact is relevant for practitioners managing  
908 supply limited systems (i.e., regulated rivers) since these conservative models may  
909 support the design of actions aiming at restoring geomorphic processes, but  
910 minimizing negative effects such as bed incision; furthermore, considering the armor  
911 condition improves the explanatory power of the bed load formulae.

912

913

914 **9 Conclusions**

915

916 This paper aims to evaluate the predictive power of 10 bed load formulae tested  
917 against bed load transport rates obtained in a large regulated river (River Ebro) that  
918 is subject to cycles of break-up and reestablishment of its armor layer. The average  
919 percentages of predicted bed load discharge that did not exceed factors of 2 ( $0.5 <$   
920  $r < 2$ ) and 10 ( $0.1 < r < 10$ ) in relation to the observed discharge were 19% and  
921 57%. This degree of discrepancy is relatively large but it is on the range observed in  
922 the literature. The P-K-M and Y formulae presented the better levels of agreement  
923 with observed bed load discharges. The formulae that performed best maintained  
924 their accuracy much more constantly over the whole range of discharges. The  
925 performance of the majority of the formulae declined when surface material is used in  
926 the BMD. It has been found that considering the armor condition improve the  
927 explanatory power of the bed load formulae. The discrepancy between predicted and  
928 observed bed load discharges was smaller in the case of the P-K-M formula than in  
929 that of Bt (the only 2 of the 10 formulae that explicitly include the effects of river  
930 bed armoring in their development). The bed load rating curve for the lower Ebro  
931 showed a similar degree of agreement to the best-performing formulae.

932

933 **Appendix A: Bed Load Transport Formulae**

934

935 **A1. Schoklitsch (1950)**

936

937  $q_{sv} = 2.5(\gamma_s/\gamma)^{-1}S^{3/2}(q - q_c)$  (A1)

938  $q_c = 0.26((\gamma_s/\gamma) - 1)^{5/3}D_{40}^{3/2}S^{-7/6}$  when  $D_{40} \geq 0.006$  m (A2)

939

940 where  $q_{sv}$  is the bed load discharge in volume per unit width ( $\text{m}^3 \cdot \text{s}^{-1} \cdot \text{m}^{-1}$ ),  $\gamma_s$  is the

941 specific weight of sediment,  $\gamma$  is the specific weight of water,  $q$  is the water discharge

942 per unit width ( $\text{m}^3 \cdot \text{s}^{-1} \cdot \text{m}^{-1}$ ),  $q_c$  is the critical water discharge per unit width

943 ( $\text{m}^3 \cdot \text{s}^{-1} \cdot \text{m}^{-1}$ ),  $S$  is the channel slope ( $\text{m} \cdot \text{m}^{-1}$ ), and  $D_{40}$  is the particle size for which

944 40% of the bed material is finer (m).

945

946 **A2. Meyer-Peter and Müller (1948)**

947

$$\left[ \frac{q_s(\gamma_s - \gamma)}{\gamma_s} \right]^{2/3} \left[ \frac{\gamma}{g} \right]^{1/3} \frac{0.25}{(\gamma_s - \gamma)D_m} = \frac{(k/k')^{3/2}\gamma RS}{(\gamma_s - \gamma)D_m} - 0.047 \quad (\text{A3})$$

948

949 where  $q_s$  is the bed load discharge in weight per unit width,  $g$  is the gravitational

950 acceleration,  $k$  is the Manning coefficient of roughness associated with skin friction

951 only,  $k'$  is the Manning coefficient of total roughness ( $k/k' = 1$ , in this study),  $R$  is

952 the hydraulic radius, and  $D_m$  is the arithmetic mean diameter.

953

954 **A3. Wong and Parker (2006)**

955

956 
$$q_{sv} = q_* \sqrt{((\gamma_s/\gamma) - 1)gD_m} D_m \quad (\text{A4})$$

957 
$$q_* = 4.93(\tau_* - 0.0470)^{1.60} \quad (\text{A5})$$

$$\tau_* = \frac{\gamma RS}{(\gamma_s - \gamma)D_m} \quad (\text{A6})$$

958

959 where  $q_{sv}$  is the bed load discharge in volume per unit width,  $q_*$  is the dimensionless  
 960 volumetric bed load transport rate per unit width, and  $\tau_*$  is the Shields number.

961

962 **A4. Einstein-Brown, Brown (1950)**

963

964 
$$q_{sv} = q_* F_1 \sqrt{((\gamma_s/\gamma) - 1)gD_{50}^3} \quad (\text{A7})$$

$$F_1 = \left[ \frac{2}{3} + \frac{36\nu^2}{g((\gamma_s - \gamma)/\gamma)D_{50}^3} \right]^{0.5} - \left[ \frac{36\nu^2}{g((\gamma_s - \gamma)/\gamma)D_{50}^3} \right]^{0.5} \quad (\text{A8})$$

965 
$$q_* = 2.15 \exp(-0.391/\tau_*) \text{ when } \tau_* < 0.09 \quad (\text{A9a})$$

966 
$$q_* = 40\tau_*^3 \text{ when } \tau_* > 0.09 \quad (\text{A9b})$$

$$\tau_* = \frac{\gamma RS}{(\gamma_s - \gamma)D_{50}} \quad (\text{A10})$$

967



968 where  $q_{sv}$  is the bed load discharge in volume per unit width,  $q_*$  is the dimensionless  
 969 volumetric bed load transport rate per unit width,  $F_1$  is the parameter of fall velocity,  
 970  $\nu$  is the kinematic viscosity of water, and  $D_{50}$  is the median particle diameter.

971

972 **A5. Ackers and White (1973), Ackers (1993)**

973

$$q_{stv} = qG_{gr} \frac{D_{35}}{y} \left[ \frac{V}{U_*} \right]^n \quad (\text{A11})$$

$$974 \quad G_{gr} = C((F_{gr}/A_{gr}) - 1)^m \quad (\text{A12})$$

$$975 \quad U_* = \sqrt{gRS} \quad (\text{A13})$$

$$F_{gr} = \frac{U_*^n}{\sqrt{gD_{35}((\gamma_s/\gamma) - 1)}} \left[ \frac{V}{\sqrt{32} \log(10y/D_{35})} \right]^{1-n} \quad (\text{A14})$$

$$D_{gr} = D_{35} \left[ \frac{g((\gamma_s/\gamma) - 1)}{\nu^2} \right]^{1/3} \quad (\text{A15})$$

976

977 for  $D_{gr} > 60$

978

$$979 \quad n = 0.0; m = 1.78; A_{gr} = 0.17; C = 0.025 \quad (\text{A16})$$

980

981 for  $1 < D_{gr} < 60$

982

$$983 \quad \log C = 2.79 \log D_{gr} - 0.98(\log D_{gr})^2 - 3.46; n = 1 - 0.56 \log D_{gr} \quad (\text{A17})$$

$$m = 1.67 + \frac{6.83}{D_{gr}}; \quad A_{gr} = 0.14 + \frac{0.23}{\sqrt{D_{gr}}} \quad (\text{A18})$$

984

985 where  $q_{stv}$  is the total bed-material load in volume per unit width,  $y$  is the mean flow  
986 depth,  $V$  is the mean flow velocity,  $U_*$  is the shear velocity,  $G_{gr}$  is the dimensionless  
987 transport rate;  $C$  is a coefficient,  $F_{gr}$  is the sediment mobilization parameter,  $A_{gr}$  is  
988 the threshold of mobility,  $D_{gr}$  is the non-dimensional sediment size,  $n$  is a transition  
989 parameter varying from 1.0 for fine material to 0 for coarse material, and  $m$  is the  
990 exponent of the transport formula.

991

## 992 **A6. Bagnold (1980)**

993

$$994 \quad q_{sm} = \frac{\rho_s}{\rho_s - \rho} q_{sr} \left[ \frac{\omega - \omega_c}{(\omega - \omega_c)_r} \right]^{3/2} \left[ \frac{y}{y_r} \right]^{-2/3} \left[ \frac{D_{50}}{D_{50r}} \right]^{-1/2} \quad (\text{A19})$$

$$995 \quad \omega = \rho y S V \quad (\text{A20})$$

$$996 \quad \omega_c = 5.75((\rho_s - \rho)D_{50}0.04)^{3/2}(g/\rho)^{1/2} \log(12y/D_{50}) \quad (\text{A21})$$

997

998 or

999

$$1000 \quad \omega_c \approx 290D_{50}^{3/2} \log(12y/D_{50}) \quad (\text{A22})$$

$$1001 \quad q_{sr} = 0.1 \text{ kg}\cdot\text{s}^{-1} \cdot \text{m}^{-1}; (\omega - \omega_c)_r = 0.5 \text{ kg}\cdot\text{s}^{-1} \cdot \text{m}^{-1}; y_r = 0.1 \text{ m}; D_{50r} = 0.0011 \text{ m} \quad (\text{A23})$$

1002

1002 where  $q_{sm}$  is the bed load discharge in mass per unit width ( $\text{kg} \cdot \text{s}^{-1} \cdot \text{m}^{-1}$ ),  $\rho_s$  is the  
1003 density of sediment ( $\text{kg} \cdot \text{m}^{-3}$ ),  $\rho$  is the density of water ( $\text{kg} \cdot \text{m}^{-3}$ ),  $\omega$  is the stream  
1004 power per unit bed area (in mass units,  $\text{kg} \cdot \text{s}^{-1} \cdot \text{m}^{-1}$ ),  $\omega_c$  is the critical unit stream  
1005 power at the beginning of movement ( $\text{kg} \cdot \text{s}^{-1} \cdot \text{m}^{-1}$ ),  $q_{sr}$  is the reference value of  $q_{sm}$   
1006 ( $\text{kg} \cdot \text{s}^{-1} \cdot \text{m}^{-1}$ ),  $(\omega - \omega_c)_r$  is the reference value of excess stream power ( $\text{kg} \cdot \text{s}^{-1} \cdot \text{m}^{-1}$ );  
1007  $y_r$  is the reference value of  $y$  (m), and  $D_{50r}$  is the reference value of  $D_{50}$  (m). Note  
1008 that in this study we have modified this equation by (1) using  $D_{50}$  instead of the  
1009 characteristic particle size in the original formulation, (2) using a fixed grain-size  
1010 rather than an event-based, and (3) using a different grain-size distribution according  
1011 to data division: surface, subsurface or combined, rather than the bed load grain-size.

1012  
1013 **A7. Yang (1984)**

1014  
1015  $q_{stw} = 10^{-3}yVC$  (A24)

1016  $C \approx C_s$  (A25)

1017  $\log C_s = 6.681 - 0.633 \log \left[ \frac{w_s D_{50}}{\nu} \right] - 4.816 \log \left[ \frac{U_*}{w_s} \right] +$   
 $+ \left\{ 2.784 - 0.305 \log \left[ \frac{w_s D_{50}}{\nu} \right] - 0.282 \log \left[ \frac{U_*}{w_s} \right] \right\} \log \left[ \frac{VS}{w_s} - \frac{V_c S}{w_s} \right]$  (A26)

1018  $U_* = \sqrt{gRS}$  (A27)

1019  $w_s = F_1(g((\gamma_s - \gamma)/\gamma)D_{50})^{0.5}$  (A28)

$$F_1 = \left[ \frac{2}{3} + \frac{36\nu^2}{g((\gamma_s - \gamma)/\gamma)D_{50}^3} \right]^{0.5} - \left[ \frac{36\nu^2}{g((\gamma_s - \gamma)/\gamma)D_{50}^3} \right]^{0.5} \quad (\text{A29})$$

1020

$$\text{for } 1.2 < \frac{U_* y}{w_s} < 70; \quad \frac{V_c}{w_s} = \frac{2.5}{\log(U_* y / \nu)} + 0.66 \quad (\text{A30})$$

1021

$$\text{for } \frac{U_* y}{w_s} \geq 70; \quad \frac{V_c}{w_s} = 2.05 \quad (\text{A31})$$

1022

1023 where  $q_{stw}$  is the total bed-material load discharge in weight per unit width  
 1024 ( $\text{kp} \cdot \text{s}^{-1} \cdot \text{m}^{-1}$ ),  $q$  is the water discharge per unit width ( $\text{m}^3 \cdot \text{s}^{-1} \cdot \text{m}^{-1}$ ),  $C$  is the total  
 1025 bed-material concentration in  $\text{mg} \cdot \text{l}^{-1}$ ,  $C_s$  is the total bed-material concentration in  
 1026 ppm by weight,  $V_c$  is the mean velocity at incipient sediment motion,  $w_s$  is the fall  
 1027 velocity of sediment, and  $F_1$  is the parameter of fall velocity.

1028

### 1029 **A8. Rottner (1959)**

1030

$$q_s = \gamma_s \sqrt{g \left[ \frac{\gamma_s - \gamma}{\gamma} \right] D_{50}^3} \left\{ \left[ \frac{2}{3} \left[ \frac{D_{50}}{y} \right]^{\frac{2}{3}} + 0.14 \right] \frac{V}{\sqrt{g \left[ \frac{\gamma_s - \gamma}{\gamma} \right] D_{50}}} - 0.778 \left[ \frac{D_{50}}{y} \right]^{2/3} \right\}^3 \quad (\text{A32})$$

1031

1032 where  $q_s$  is the bed load discharge in weight per unit width.

1033

1034 **A9. Parker et al. (1982)**

1035

1036  $q_{sv} = W^*(yS)^{1.5}g^{0.5}((\gamma_s/\gamma) - 1)^{-1}$  (A33)

1037

1038 for  $0.95 < \varphi_{50} < 1.65$ ;  $W^* = 0.0025 \exp(14.2(\varphi_{50} - 1) - 9.28(\varphi_{50} - 1)^2)$  (A34)

1039

1040 for  $\varphi_{50} > 1.65$ ;  $W^* = 11.2(1 - (0.822/\varphi_{50}))^{4.5}$  (A35)

1041

1042  $\varphi_{50} = \tau_{50}^*/\tau_{r50}^*$  (A36)

1043  $\tau_{50}^* = \frac{\gamma y S}{(\gamma_s - \gamma) D_{50s}}$ ;  $\tau_{r50}^* = 0.0876$  (A37)

1044

1044 where  $q_{sv}$  is the bed load in volume per unit width,  $W^*$  is the dimensionless bed load,

1045  $D_{50s}$  is the median diameter of subsurface material,  $\tau_{50}^*$  is the Shields stress for  $D_{50s}$ ,

1046  $\tau_{r50}^*$  is the reference value of  $\tau_{50}^*$ , and  $\varphi_{50}$  is the excess Shields stress.

1047

1048 **A10. Bathurst (2007)**

1049

1050  $q_{sm} = a\rho(q - q_{c2})$  (A38)

1051  $a = 29.2S^{1.5}(D_{50}/D_{50s})^{-3.30}$  (A39)

1052  $q_{c2} = 0.5(0.0513g^{0.5}D_{50}^{1.5}S^{-1.20} + 0.0133g^{0.5}D_{84}^{1.5}S^{-1.23})$  (A40)

1053

1054 where  $q_{sm}$  is the bed load discharge in mass per unit width ( $\text{kg} \cdot \text{s}^{-1} \cdot \text{m}^{-1}$ ),  $q$  is the  
1055 water discharge per unit width ( $\text{m}^3 \cdot \text{s}^{-1} \cdot \text{m}^{-1}$ ),  $q_{c2}$  is the threshold or critical water  
1056 discharge per unit width for transport of material as the armor layer breaks up  
1057 ( $\text{m}^3 \cdot \text{s}^{-1} \cdot \text{m}^{-1}$ ),  $a$  is a dimensionless coefficient that represent the rate of change of bed  
1058 load discharge with water mass discharge,  $\rho$  is the water density ( $\text{kg} \cdot \text{m}^{-3}$ ),  $D_{50s}$  is  
1059 the median diameter of subsurface material (m),  $D_{84}$  is the particle size of percentile  
1060 84 of surface layer material (m),  $g$  is the gravitational acceleration ( $\text{m} \cdot \text{s}^{-2}$ ), and  $S$  is  
1061 the channel slope ( $\text{m} \cdot \text{m}^{-1}$ ).

1062

1063 **Notation**

1064

1065  $a$  dimensionless coefficient.

1066  $A_{gr}$  threshold of mobility.

1067  $C$  coefficient.

1068  $C_s$  total bed-material concentration, ppm by weight.

1069  $D_i$  particle size of percentile  $i$ , m.

1070  $D_{ir}$  reference value of  $D_i$ , m.

1071  $D_{is}$  particle size of percentile  $i$  of subsurface material, m.

1072  $D_{gr}$  non-dimensional sediment size, m.

1073  $D_m$  arithmetic mean diameter of sediment, m.

1074  $F_1$  adimensional parameter of fall velocity.

1075  $F_{gr}$  sediment mobilization parameter.

1076  $g$  gravitational acceleration,  $\text{m} \cdot \text{s}^{-2}$ .

1077  $gr$  modified geometric mean value of  $r$ .

1078  $gwr$  weighted variation of  $gr$ .

1079  $G_{gr}$  dimensionless transport rate.

1080  $k$  Manning coefficient of roughness associated with skin friction only,  $\text{s} \cdot \text{m}^{-1/3}$ .

1081  $k'$  Manning coefficient of total roughness,  $\text{s} \cdot \text{m}^{-1/3}$ .

1082  $m$  exponent.

1083  $mr$  mean of discrepancy ratio ( $r$ ).

1084	$mlr$	mean of logarithm of discrepancy ratio ( $r$ ).
1085	$mq_{sp}$	minimum value of $q_{sp}$ .
1086	$n$	transition parameter.
1087	$N$	number of data.
1088	$Q$	water discharge, $m^3 \cdot s^{-1}$ .
1089	$q_c$	critical water discharge per unit width, $m^3 \cdot s^{-1} \cdot m^{-1}$ .
1090	$q_{c2}$	critical water discharge per unit width for transport as the armor layer
1091		breaks up, $m^3 \cdot s^{-1} \cdot m^{-1}$ .
1092	$q_s$	bed load discharge in weight per unit width, $N \cdot s^{-1} \cdot m^{-1}$ .
1093	$q_{sm}$	bed load discharge in mass per unit width, $kg \cdot s^{-1} \cdot m^{-1}$ .
1094	$q_{so}$	observed bed load discharge per unit width, $N \cdot s^{-1} \cdot m^{-1}$ .
1095	$q_{sp}$	predicted bed load discharge per unit width, $N \cdot s^{-1} \cdot m^{-1}$ .
1096	$q_{sr}$	reference value of $q_{sm}$ , $kg \cdot s^{-1} \cdot m^{-1}$ .
1097	$q_{stv}$	total bed-material load discharge in volume per unit width, $m^3 \cdot s^{-1} \cdot m^{-1}$ .
1098	$q_{stw}$	total bed-material load discharge in weight per unit width, $kp \cdot s^{-1} \cdot m^{-1}$ .
1099	$q_{sv}$	bed load discharge in volume per unit width, $m^3 \cdot s^{-1} \cdot m^{-1}$ .
1100	$q^*$	dimensionless volumetric bed load transport rate per unit width.
1101	$r$	discrepancy ratio ( $q_{sp}/q_{so}$ ).
1102	$rw$	weighted value of $r$ .
1103	$R$	hydraulic radius, m.
1104	$S$	bed or channel slope, $m \cdot m^{-1}$ .



1105	$U_*$	shear velocity, $\text{m} \cdot \text{s}^{-1}$ .
1106	$V$	mean flow velocity, $\text{m} \cdot \text{s}^{-1}$ .
1107	$V_c$	critical mean velocity, $\text{m} \cdot \text{s}^{-1}$ .
1108	$w_s$	fall velocity of sediment, $\text{m} \cdot \text{s}^{-1}$ .
1109	$W^*$	dimensionless bed load.
1110	$y$	mean flow depth, $\text{m}$ .
1111	$y_r$	reference value of $y$ , $\text{m}$ .
1112	$\phi_i$	excess Shields stress.
1113	$\gamma$	specific weight of water, $\text{N} \cdot \text{m}^{-3}$ .
1114	$\gamma_s$	specific weight of sediment, $\text{N} \cdot \text{m}^{-3}$ .
1115	$\nu$	kinematic viscosity of water, $\text{m}^2 \cdot \text{s}^{-1}$ .
1116	$\rho$	density of water, $\text{kg} \cdot \text{m}^{-3}$ .
1117	$\rho_s$	density of sediment, $\text{kg} \cdot \text{m}^{-3}$ .
1118	$\tau$	mean shear stress, $\text{N} \cdot \text{m}^{-2}$ .
1119	$\tau^*$	Shields number.
1120	$\tau_i^*$	Shields stress for $D_{is}$ .
1121	$\tau_{ri}^*$	reference value of $\tau_i^*$ .
1122	$\omega$	stream power per unit bed area, $\text{kg} \cdot \text{s}^{-1} \cdot \text{m}^{-1}$ .
1123	$\omega'$	stream power per unit weight of fluid, $\text{m} \cdot \text{s}^{-1}$ .
1124	$\omega_c$	critical unit stream power, $\text{kg} \cdot \text{s}^{-1} \cdot \text{m}^{-1}$ .
1125	$(\omega - \omega_c)_r$	reference value of excess stream power, $\text{kg} \cdot \text{s}^{-1} \cdot \text{m}^{-1}$ .
1126		

1127 **Acknowledgements**

1128

1129 This research was carried out within the framework of the research projects  
1130 REN2001-0840-C02-01/HID, CGL2005-06989-C02-02/HID, CGL2006-11679-C02-  
1131 01/HID, CGL2009-09770 (subprograma BTE), and SCARCE Consolider Ingenio 2010  
1132 CSD2009-00065, all funded by the Spanish Ministry of Science and Technology. The  
1133 second author has benefit from a Juan de la Cierva Fellowship (JCI-2008-2910)  
1134 funded by the Spanish Ministry of Science and Innovation and a Ramon y Cajal  
1135 Fellowship (RYC-2010-06264) funded by the Spanish Ministry of Science and  
1136 Innovation. Hydrological data were supplied by the Ebro Water Authorities. The  
1137 Móra d'Ebre Town Council provided logistical support during fieldwork. Albert  
1138 Rovira assisted during fieldwork and labwork. Comments by Jonathan B. Laronne,  
1139 John Buffington and anonymous reviewers were extremely helpful in improving the  
1140 manuscript.

1141

1142 **References**

1143

1144 Ackers, P., 1993. Sediment transport in open channels: Ackers and White update.

1145 Proc. Inst. Civ. Engrs. Wat., Marit. Energ. 101, 247–249.

1146 Ackers, P., White W.R., 1973. Sediment transport: New approach and analysis. J.

1147 Hydraul. Div. 99(11), 2041–2060.

1148 Andrews, E.D., 1981. Measurement and computation of bed material discharge in a

1149 shallow sand-bed stream, Muddy Creek, Wyoming. Water Resour. Res. 17, 131–141.

1150 Bagnold, R.A., 1980. An empirical correlation of bed load transport rates in flumes

1151 and natural rivers. Proc. R. Soc. London Ser. A. 372, 453–473.

1152 Barry, J.J., Buffington, J.M., King J.G., 2004. A general power equation for

1153 predicting bed load transport rates in gravel bed rivers. Water Resour. Res. 40,

1154 W10401, doi:10.1029/2004WR003190.

1155 Barry, J.J., Buffington, J.M., King J.G., 2007. Correction to “A general power

1156 equation for predicting bed load transport rates in gravel bed rivers”. Water Resour.

1157 Res. 43, W08702, doi:10.1029/2007WR006103.

1158 Barry, J.J., Buffington, J.M., Goodwin, P.G., King, J.G., Emmett, W.W., 2008.

1159 Performance of bed-load transport equations relative to geomorphic significance:

1160 Predicting effective discharge and its transport rate. J. Hydraul. Eng. 134(5), 601–

1161 615.

1162 Batalla, R.J., 1997. Evaluating bed-material transport equations from field  
1163 measurements in a sandy gravel-bed river. *Earth Surf. Proc. Land.* 21, 121–130.

1164 Batalla, R.J., Vericat, D., 2009. Hydrological and sediment transport dynamics of  
1165 flushing flows: Implications for management in large Mediterranean rivers. *River Res.*  
1166 *Applic.* 25, 297–314.

1167 Batalla, R.J., Gomez, C.M., Kondolf, G.M., 2004. Reservoir-induced hydrological  
1168 changes in the Ebro River basin (Northeastern Spain). *J. Hydrol.* 290, 1–2, 117–136.

1169 Bathurst, J.C., 2007. Effect of coarse surface layer on bed-load transport. *J. Hydraul.*  
1170 *Eng.* 133(11), 1192–1205.

1171 Brown, C.B., 1950. Sediment transportation, in: Rouse, H. (Ed.), *Engineering*  
1172 *Hydraulics*. Wiley, New York, pp. 769–857.

1173 Carson, M.A., Griffith, G.S., 1987. Bed load transport in gravel channels. *J. Hydrol.*  
1174 (NZ) 26(1), 1–151.

1175 Casey, H.J., 1935. Über geschiebebewegung, *Mitteilungen der Preussischen*  
1176 *Versuchsanstalt*  
1177 *für Wasserbau und Schiffbau.* 19, 86 pp.

1178 Chang, Y.L., 1939. Laboratory investigation of flume traction and transportation,  
1179 *Transactions of the American Society of Civil Engineers.* 104, 1246-1284.

1180 Chang, H.H., 1988. *Fluvial Processes in River Engineering*, Wiley, New York.

1181 Chang, H.H., 1994. Selection of gravel-transport formula for stream modeling. *J.*  
1182 *Hydraul. Eng.* 120(5), 646–651.

1183 Church, M., McLean, D.G., Wolcott, J.F., 1987. River bed gravels: sampling and  
1184 analysis. In: Thorne, C.R., Barthurst, J.C., Hey, R.D. (Eds.), *Sediment Transport in*  
1185 *Gravel-bed Rivers*. John Wiley and Sons, Chichester, UK, pp. 43–88.

1186 Dietrich, W.E, Kirchner, J.W., Ikeda, H., Iseya F., 1989. Sediment supply and the  
1187 development of the coarse surface layer in gravel-bedded rivers. *Nature*. 340, 215-217.

1188 Di Cristo, C., Iervolino, M., Vacca A., 2006. Linear stability analysis of a 1-D model  
1189 with dynamical description of bed-load transport. *J. Hydraul. Res.* 44(4), 480–487.

1190 Duan, J.G., Chen, L., Scott, S., 2006. Application of surface-based bed load transport  
1191 equations to a desert gravel-bed stream. *J. Hydraul. Res.* 44(5), 624–630.

1192 Ferguson, R.I., 2003. The missing dimension: effects of lateral variation on 1-D  
1193 calculations of fluvial bedload transport. *Geomorphology* 56, 1–14.

1194 Fripp, J.B., Diplas, P., 1993. Surface sampling in gravel streams. *J. Hydraul. Eng.*  
1195 119(4), 473–490.

1196 Gilbert, G.K., 1914. *The transportation of débris by running water*. U.S. Geological  
1197 Survey Professional Paper 86, 263 pp.

1198 Gomez, B., 2006. The potential rate of bed-load transport. *PNAS* 103(46), 17170–  
1199 17173.

1200 Gomez, B., Church, M., 1989. Assessment of bed load sediment transport formulae  
1201 for gravel bed rivers. *Water Resour. Res.* 25(6), 1161–1186.

1202 Greco M., Iervolino M., Leopardi A., Vacca A., 2012. A two-phase model for fast  
1203 geomorphic shallow flows. *Int. J. Sediment Res.* 27(4), 409–425.

1204 Habersack, H., Laronne, J.B., 2002. Evaluation and improvement of bed load  
1205 discharge formulas based on Helley–Smith sampling in an Alpine gravel bed river. *J.*  
1206 *Hydraul. Eng.* 128(5), 484–499.

1207 Hamamori, A., 1962. A theoretical investigation on the fluctuations of bed load  
1208 transport. Report R4, 14 pp., Delft Hydraulics Laboratory, Delft, The Netherlands.

1209 Johnson, J.W., 1939. Discussion of ‘Laboratory investigation of flume traction and  
1210 transportation’. *Trans. Am. Soc. Civ. Eng.* 104, 1247–1313.

1211 Julien, P.Y., 1998. *Erosion and Sedimentation*, Cambridge University Press, New  
1212 York.

1213 Kellerhals, R., Bray, D.I., 1971. Sampling procedures for coarse fluvial sediments. *J.*  
1214 *Hydraul. Div.* 97(8), 1165–1180.

1215 Kramer, H., 1934. Sand mixtures and sand movements in fluvial models. Proceedings  
1216 of the American Society of Civil Engineers 60(4), 443–483.

1217 Lane, E.W., Carlson, E.J., 1953. Some factors affecting the stability of canals  
1218 constructed in coarse granular materials. Proceedings of the 5th Congress IAHR,  
1219 Delf, The Netherlands.

1220 López, R., Justribó, C., 2010. The hydrological significance of mountains: a regional  
1221 case study, the Ebro River basin, northeast Iberian Peninsula. *Hydrol. Sci. J.* 55(2),  
1222 223–233.

1223 Martin, Y., 2003. Evaluation of bed load transport formulae using field evidence from  
1224 the Vedder River, British Columbia. *Geomorphology* 53, 75–95.

1225 Martin, Y., Ham, D., 2005. Testing bed load transport formulae using morphologic  
1226 transport estimates and field data: lower Fraser River, British Columbia. *Earth Surf.*  
1227 *Proc. Land.* 30, 1265–1282.

1228 Meyer-Peter, E., Müller, R., 1948. Formulas for bed-load transport. *Proc. 2nd*  
1229 *Meeting of the Int. Assoc. for Hydraulic Structures Res.* pp. 39–64, IAHR, Delft, The  
1230 Netherlands.

1231 Parker, G., 1990. Surface-based bedload transport relation for gravel rivers. *J.*  
1232 *Hydraul. Res.* 28, 417–436.

1233 Parker, G., Klingeman, P.C., 1982. On why gravel bed streams are paved. *Water*  
1234 *Resour. Res.* 18 (5), 1409–1423.

1235 Parker, G., Klingeman, P.C., McLean, D.G., 1982. Bedload and the size distribution  
1236 of paved gravel-bed streams. *J. Hydraul. Div.* 108(4), 544–571.

1237 Recking, A., 2010. A comparison between flume and field bed load transport data  
1238 and consequences for surfacebased bed load transport prediction. *Water Resour. Res.*  
1239 46, W03518, doi:10.1029/2009WR008007.

1240 Reid, I., Powell, D.M., Laronne J.B., 1996. Prediction of bed load transport by desert  
1241 flash-floods. *J. Hydraul. Eng.* 122(3), 170–173.

1242 Rice, S., Church, M., 1996. Sampling surficial fluvial gravels: the precision of size  
1243 distribution percentile estimates. *J. Sediment. Res.* 66(3), 654–665.

1244 Rice, S.P., Haschenburger, J.K., 2004. A hybrid method for size characterization of  
1245 coarse subsurface fluvial sediments. *Earth Surf. Proc. Land.* 29, 373–389.

1246 Rottner, J., 1959. A formula for bed load transportation. *La Houille Blanche* 3(4),  
1247 301–307.

1248 Shields, A., 1936. Anwendung der Aehnlichkeitsmechanik und der  
1249 Turbulenzforschung auf die Geschiebebewegung, *Mitteilungen der Preussischen*  
1250 *Versuchsanstalt für Wasserbau und*  
1251 *Schiffbau*, 26, 26 pp.

1252 Schoklitsch, A., 1950. *Handbuch des wasserbaues*, Springer, New York.

1253 Shulits, S., Hill, R.D., 1968. Bed load formulas. Rep. No. ARSSCW-1, Agricultural  
1254 Research Services, USDA, Washington.

1255 Turowski, J.M., Badoux, A., Rickenmann, D., 2011. Start and end of bed load  
1256 transport in gravel-bed streams. *Geophys. Res. Lett.* 38, L04401.

1257 USACE, 1989. Sedimentation investigations of rivers and reservoirs. Engineer Manual  
1258 1110-2-4000, Department of the Army, U.S. Army Corps of Engineers, Washington.

1259 USWES, 1935. Study of river-bed material and their use with special reference to the  
1260 lower Mississippi River. United States Waterways Experiment Station, Vicksburg,  
1261 MS. Paper 17, 161 pp.

1262 Vericat, D., Batalla, R.J., 2005. Bed load variability under low sediment transport  
1263 conditions in the lower Ebro River (NE Spain), in: Batalla, R.J., Garcia, C. (Eds.),  
1264 *Geomorphological Processes and Human Impacts in Rivers Basins*. Wallingford, IAHS  
1265 Publication n°299, pp. 173–180.



1266 Vericat, D., Batalla, R.J., 2006. Sediment transport in a large impounded river: The  
1267 lower Ebro, NE Iberian Peninsula. *Geomorphology* 79, 72–92.

1268 Vericat, D., Batalla, R.J., Garcia, C., 2006a. Breakup and reestablishment of the  
1269 armor layer in a highly regulated large gravel-bed river: the lower Ebro.  
1270 *Geomorphology* 76, 122–136.

1271 Vericat, D., Church, M., Batalla, R.J., 2006b. Bed load bias: Comparison of  
1272 measurements obtained using two (76 and 152 mm) Helley-Smith samplers in a  
1273 gravel-bed river. *Water Resour. Res.* W01402, doi:10.1029/2005WR004025.

1274 White, W.R., Milli, H., Crabbe, A.D., 1973. Sediment transport: an appraisal of  
1275 available methods, Rep. 119, UK Hydraulics Research Station, Wallingford, UK.

1276 White, W.R., Milli, H., Crabbe, A.D., 1975. Sediment transport theories: a review, P.  
1277 I. *Civil Eng.* 59(2), 265–292.

1278 Wilcock, P.R., 2001. The flow, the bed, and the transport: Interaction in flume and  
1279 field, in: Mosley, M.P. (Ed.), *Gravel-Bed Rivers V*. NZHS, Wellington, NZ., pp. 183-  
1280 219.

1281 Wolman, M.G., 1954. A method of sampling coarse bed material. *Am. Geophys. Union*  
1282 *Trans.* 35, 951–956.

1283 Wong, M., Parker, G., 2006. Reanalysis and correction of bed-load relation of Meyer-  
1284 Peter and Müller using their own database. *J. Hydraul. Eng.* 132(11), 1159–1168.

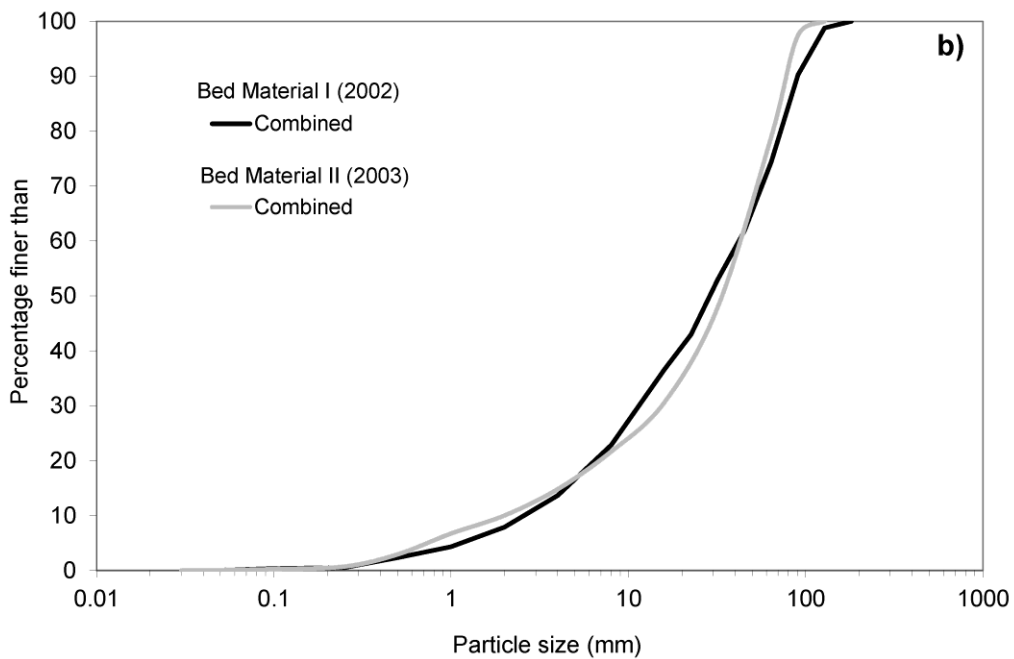
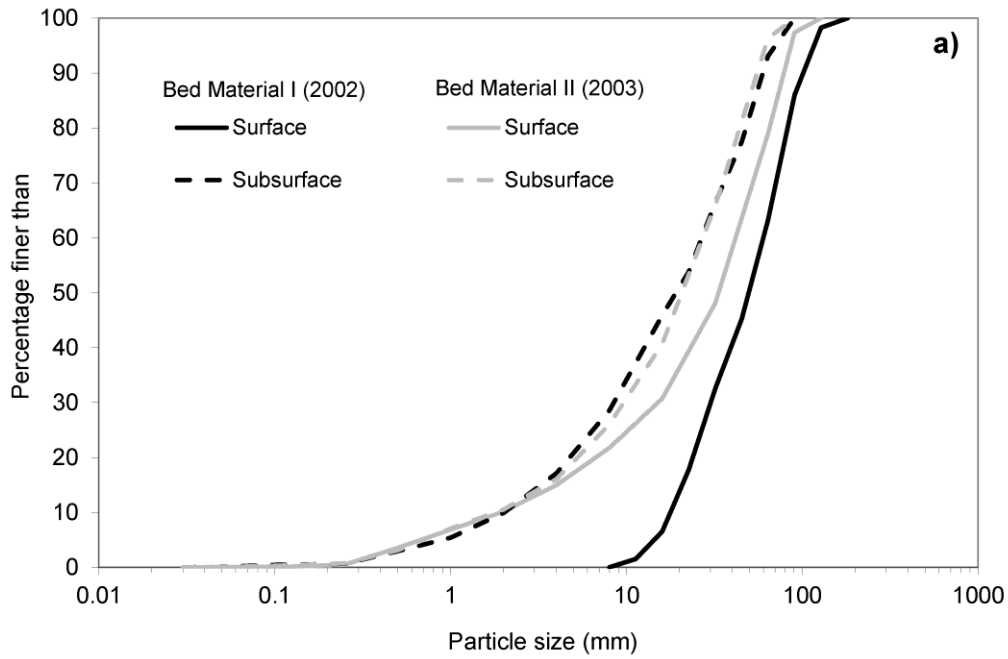
1285 Yang, C.T., 1973. Incipient motion and sediment transport. *J. Hydraul. Div.* 99(10),  
1286 1679–1704.

1287 Yang, C.T., 1984. Unit stream power equation for gravel. J. Hydraul. Div. 110(12),  
1288 1783–1797.

1289 Yang, C.T., Wan, S., 1991. Comparisons of selected bed-material load formulas. J.  
1290 Hydraul. Eng. 117(8), 973–989.

1291

Accepted Version



1292

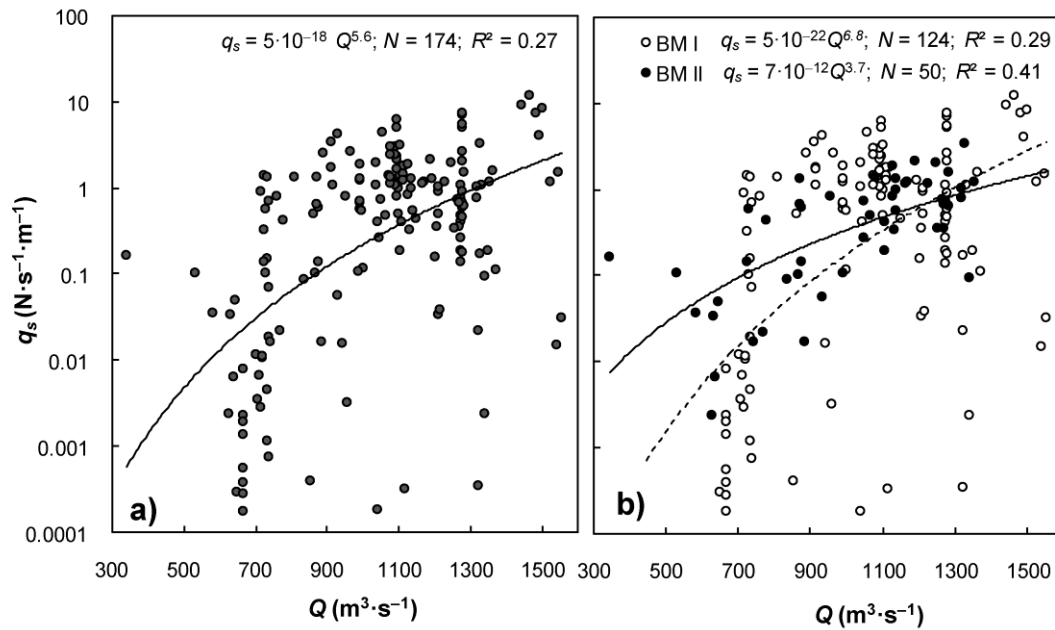
1293 Figure 1. Bed material grain-size distributions at an exposed bar 500 m downstream

1294 from the MEMS: (a) surface and subsurface grain-size distributions of Bed Material I

1295 (BMI, obtained in 2002) and Bed Material II (BMII, obtained in 2003), and (b)

1296 combined distribution (surface and subsurface materials) for each sampling period

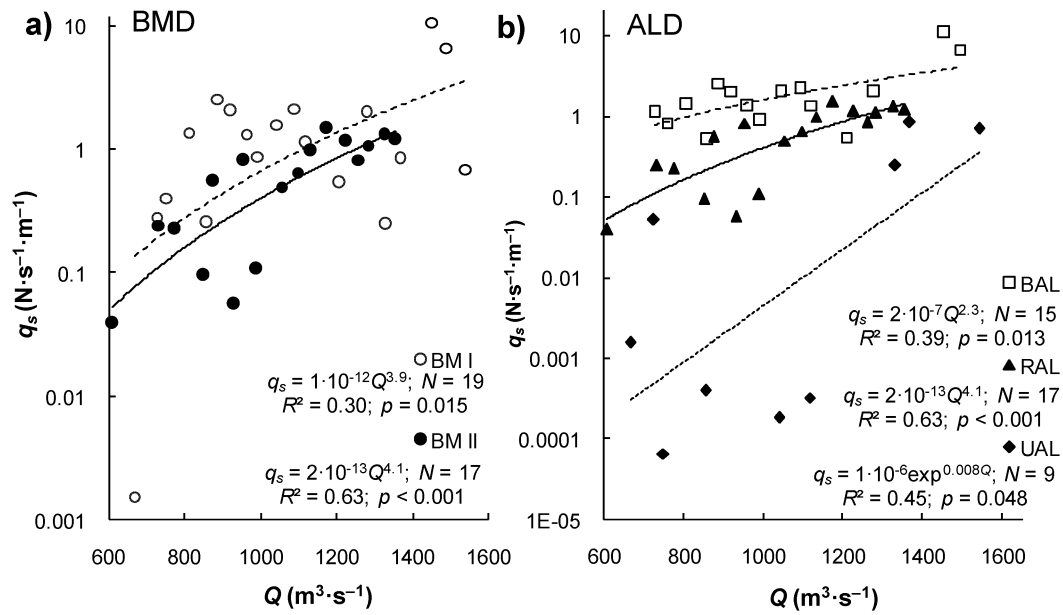
1297 (BMI and BMII). Statistics are summarized in Table 1 (see methods in the text).



1298

1299 Figure 2. Relation between observed unit bed load discharge and water discharge: (a)  
 1300 original database, and (b) original database divided by bed material: Bed Material I  
 1301 (BMI, bed load samples between summer 2002 and summer 2003) and Bed Material  
 1302 II (BMII, samples after summer 2003).

1303



1304

1305 Figure 3. Relation between average unit bed load discharge and water discharge. (a)

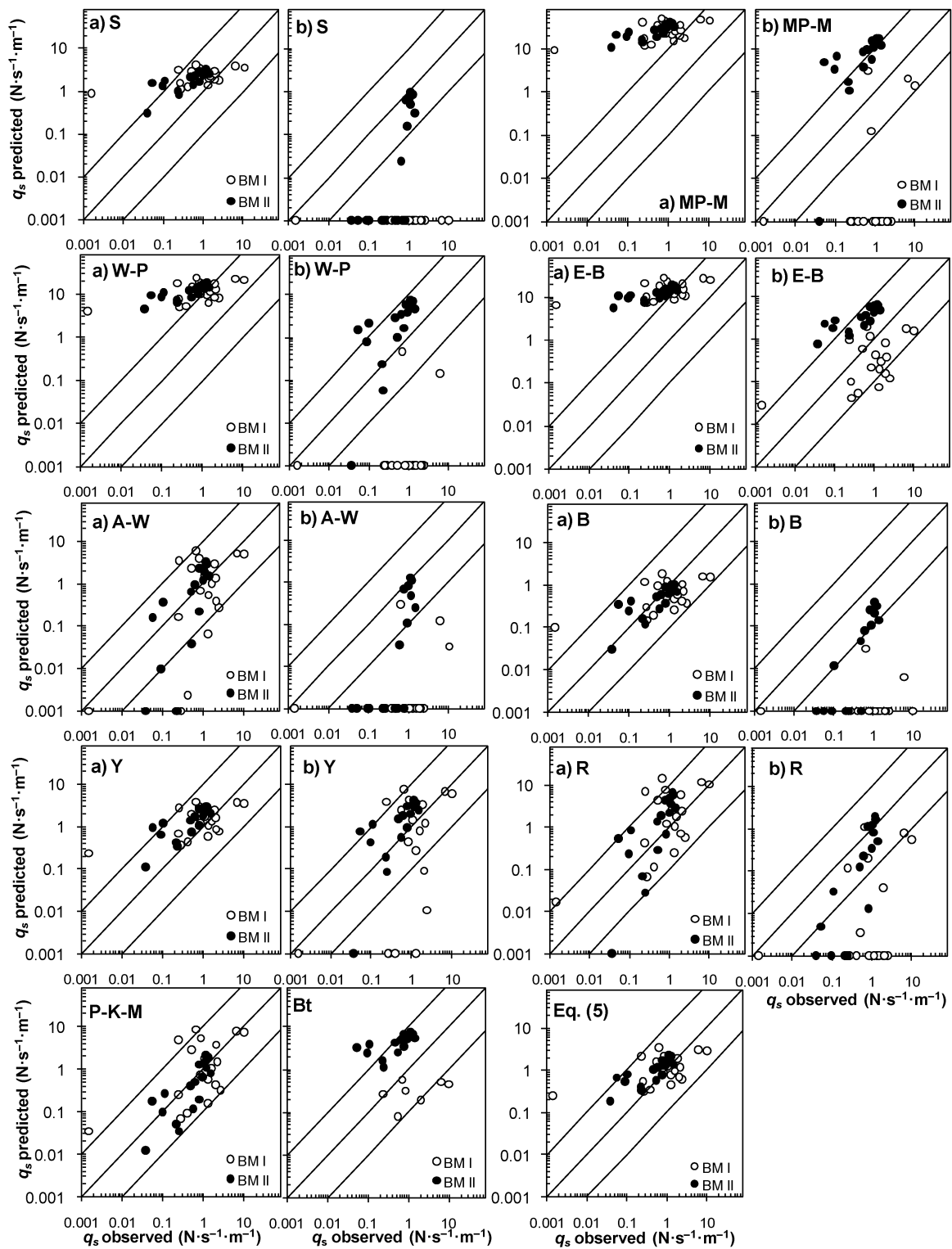
1306 Data divided by bed material (BMI and BMII) classes and grouped by discharge

1307 bins: Bed Material Division (BMD). (b) Data divided by armor integrity and

1308 grouped by discharge bins: Armor Layer Division (ALD). (See section 4.2 for more

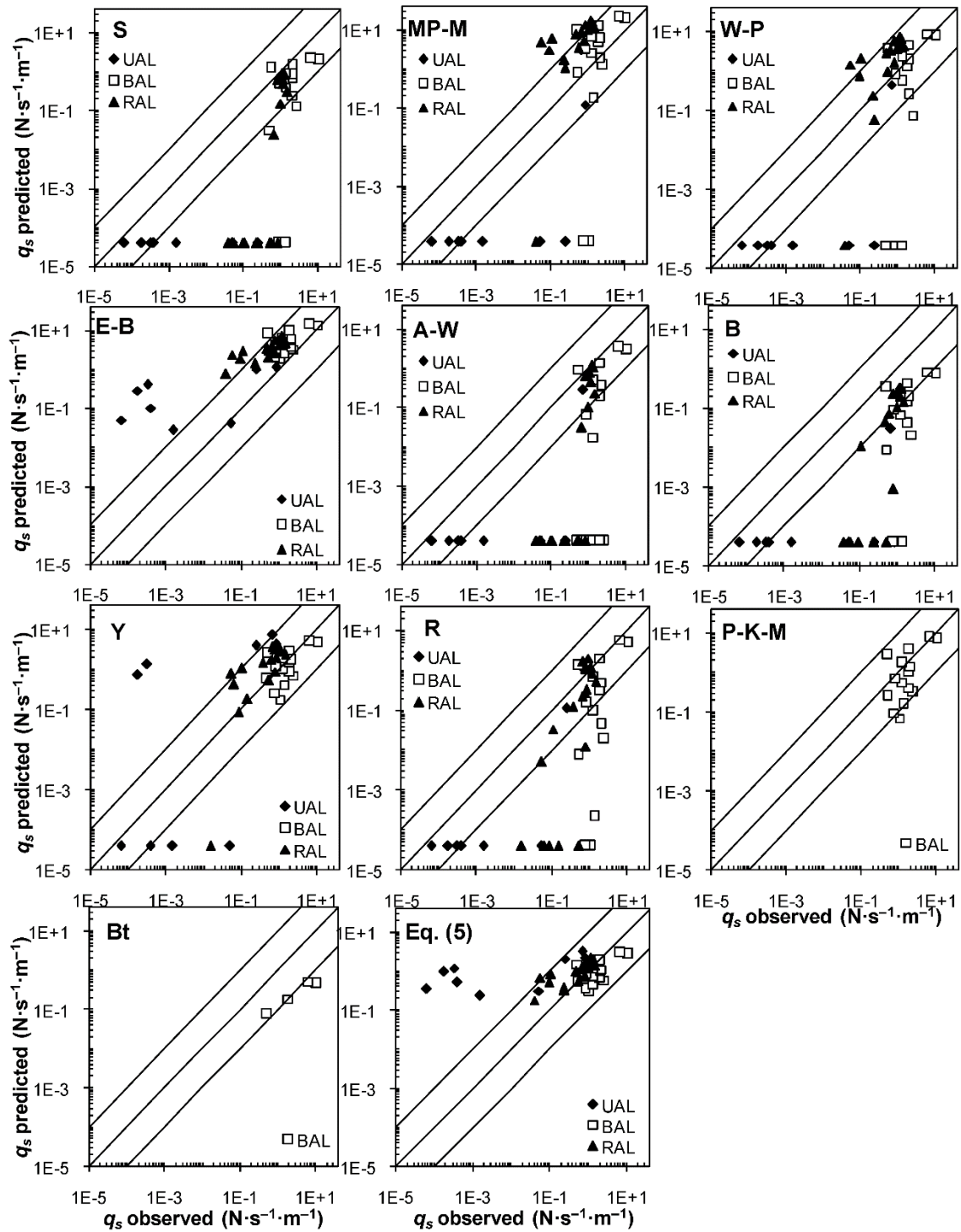
1309 details about data sets grouping and division).

1310



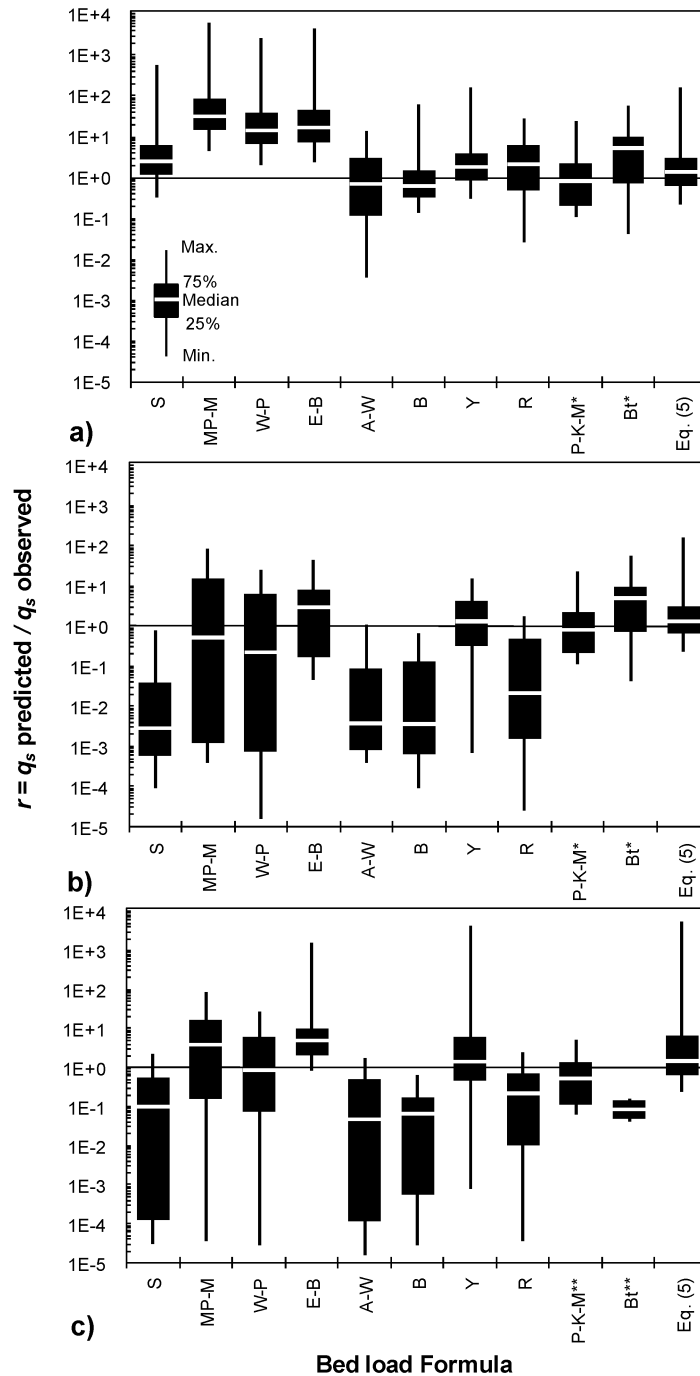
1311

1312 Figure 4. Predicted unit bed load discharge using selected formulae plotted against observed rates  
 1313 according to the Bed Material Division (BMD) and using (a) subsurface bed material and (b) surface  
 1314 bed material. Note that the P-K-M and Bt formulae directly specify the (surface and/or subsurface)  
 1315 material required to predict bed load discharge. Lines parallel to the line of perfect equality ( $r = 1$ )  
 1316 correspond to  $r = 0.1$  and  $r = 10$ . Values plotted on the  $x$  axis correspond to bed load zero predictions.  
 1317



1318

1319 Figure 5. Predicted unit bed load discharge by evaluated formulas plotted against observed  
 1320 rates according to the Armor Layer Division (ALD); i.e., UAL: unbroken armor layer, BAL:  
 1321 broken armor layer, and RAL: reestablished armor layer. Lines parallel to the line of perfect  
 1322 equality ( $r = 1$ ) correspond to  $r = 0.1$  and  $r = 10$ . Values plotted parallel to the  $x$  axis  
 1323 correspond to bed load zero predictions.  
 1324



1325

1326

1327

1328

1329

1330

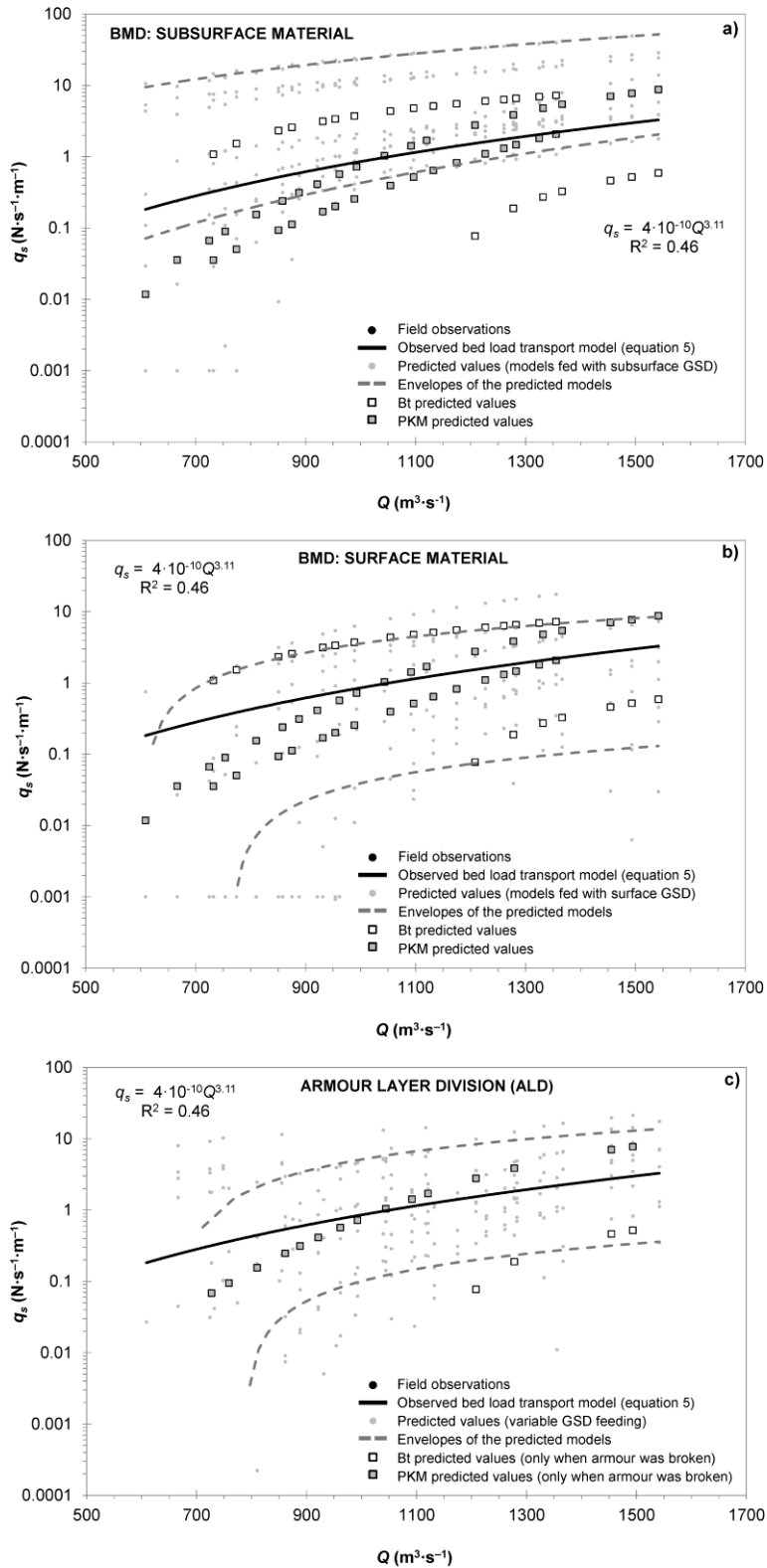
1331

1332

1333

Figure 6. Box plots of the distribution of the ratio between predicted and observed unit bed load discharge according to data sets: (a) Bed Material Division (BMD) data fed by subsurface bed material; (b) Bed Material Division (BMD) data fed by surface bed material; and (c) Armor Layer Division (ALD). Note that (\*) indicates that the P-K-M and Bt formulae directly specify the (surface and/or subsurface) material required to predict bed load discharge; likewise formulae with (\*\*) indicates that only BAL data was used (see section 4.3 for more details).





1334

1335 Figure 7. Summary of model performance for the different bed material division (BMI  
 1336 and BMII) and armoring conditions (ALD). The observed bed load average model  
 1337 (Eq. (5)) is highlighted for reference.

1338

1339 Table 1. Grain Size Percentiles of Surface, Subsurface and Combined River Bed  
 1340 Material observed in the Lower Ebro River (500 m downstream from the monitoring  
 1341 site; see Figure 1 for the complete Grain Size Distributions).

1342

Grain size $D_i$ (mm)	Bed material I (BMI) <sup>a</sup>			Bed material II (BMII) <sup>c</sup>		
	Subsurface	Surface	Combined <sup>b</sup>	Subsurface	Surface	Combined <sup>d</sup>
$D_{35}$	10	34	15	12	19	19
$D_{40}$	13	39	19	15	23	23
$D_{50}$	19	50	29	21	33	33
$D_m$	26	55	40	26	38	38
$D_{84}$	52	88	79	48	70	70

1343

1344 <sup>a</sup> Sampling was conducted before the flood season; BMI: characterization  
 1345 performed in 2002, at the beginning of the 2002-2003 hydrological year.

1346 <sup>b</sup> Combined grain-size distribution has been calculated according to Fripp and  
 1347 Diplas (1993) and Rice and Haschenburger (2004)

1348 <sup>c</sup> BMII: characterization performed in 2003, at the beginning of the 2003-2004  
 1349 hydrological year.

1350 <sup>d</sup> Fines were significant on the surface in summer 2003. Surface material was  
 1351 sampled by means of the area by weight approach, a sample that represents  
 1352 the full range of sizes in the bed. Percentiles for the surface and combined  
 1353 distributions are almost identical because the weight of the subsurface material  
 1354 on the combined one.

1355 Table 2. Characteristics of the Selected Bed Load Transport Formulae

1356

Formula	Name or reference	Load	Theoretical approach	Environment of the data	$N^a$	Experimental range
S	Schoklitsch (1950)	Bed load	Discharge	Flume, field	—	$0.3 < S(\%) < 10$
MP-M	Meyer-Peter and Müller (1948)	Bed load	Shear stress	Flume	251	$0.040 < S(\%) < 2.0$ $0.38 < D_m(\text{mm}) < 28.65$
W-P	Wong and Parker (2006)	Bed load	Shear stress	Flume	168	$3.17 < D_m(\text{mm}) < 28.65$
E-B	Einstein-Brown, Brown (1950)	Bed load	Probabilistic	Flume	—	$0.3 < D_{50}(\text{mm}) < 28.6$
A-W	Ackers and White (1973), Ackers (1993)	Total load <sup>b</sup>	Stream power	Flume	$\approx 1000$	$0.04 < D(\text{mm}) < 4$ $F < 0.8$
B	Bagnold (1980)	Bed load	Stream power	Flume, field	—	$0.3 < D_{50}(\text{mm}) < 300$
Y	Yang (1984)	Total load <sup>b</sup>	Stream power	Flume	167	$2.5 < D(\text{mm}) < 7.0$
R	Rottner (1959)	Bed load	Regression	Flume, field	$\approx 2500$	$0.31 < D_{50}(\text{mm}) < 15.5$
P-K-M	Parker et al. (1982)	Bed load	Probabilistic, equal mobility	Field	—	$D_{50\ s} < 28 \text{ mm}$
Bt	Bathurst (2007)	Bed load	Discharge	Field	$\approx 600$	$0.048 < S(\%) < 4.8$ $12 < D_{50}(\text{mm}) < 146$ $30 < D_{84}(\text{mm}) < 540$ $1.52 < D_{50}/D_{50\ s} < 11$

1357

<sup>a</sup> Number of calibration data.

1358

<sup>b</sup> Total bed-material load.

1359

1360 Table 3. Schematic Division of the Data Performed in this Study. Two Main Analyses were Performed: a) Based on the Raw Data and  
 1361 b) Based on Data Division. Data Division was based on Bed Material Characteristics and on the Armor Layer Integrity

		RAW DATA			DATA DIVISION		
		BED MATERIAL SAMPLES $N = 2$	BED LOAD SAMPLES $N = 174$	BED MATERIAL DIVISION	DISCHARGE CLASSES $N = 21$	BED MATERIAL DIVISION (BMD)	ARMOR LAYER DIVISION (ALD)
2002-2003	Bed Material I (BMI)	Sample 1	...	BMI	$Q_1 (Q_1 < 700$	BMI	Unbroken Armor Layer (UAL)
		Sample 2			$Q_2 (Q_1 - Q_{1+j})$		
	...	...			...		Broken Armor Layer (BAL)
	<i>High magnitude floods</i>	...			...		
	Sample 124	...			...		
2003-2004	Bed Material II (BMII)	Sample 125	...	BMII	...	BMII	Reestablished Armor Layer (RAL)
		Sample 126			...		
	...	...			...		
	<i>Low magnitude floods</i>	...			...		
	Sample 174	...			$Q_n (Q_{1+k} - Q_{1+k+j})$		

1362 Table 4. Data Division: Number of data in each subset (see section 4 for more details)

1363

Original database	Data Division						
	Bed Material		Grouping Discharges				
	Bed Material I	Bed Material II	Bed Material Division (BMD)		Armor Layer Division (ALD)		
			BMI <sup>b</sup>	BMII <sup>c</sup>	UAL <sup>d</sup>	BAL <sup>e</sup>	RAL <sup>f</sup>
$N^a = 174$	$N = 124$	$N = 50$	$N = 19$	$N = 17$	$N = 9$	$N = 15$	$N = 17$

1364

1365 <sup>a</sup>Number of data.

1366 <sup>b</sup>BMI, Bed Material I, river bed grain size distributions obtained in 2002.

1367 <sup>c</sup>BMII, Bed Material II, river bed grain size distributions obtained in 2003.

1368 <sup>d</sup>UAL, Unbroken Armor Layer condition.

1369 <sup>e</sup>BAL, Broken Armor Layer condition.

1370 <sup>f</sup>RAL, Reestablished Armor Layer condition.

1371

1372 Table 5. Comparison of the predictive power of the formulae according to the Bed Material Division (BMD) and using the subsurface bed material  
 1373 to feed the formulae. Note that results are sorted from best to worst performance according to each index. In bold the formulae ranked in the first  
 1374 four positions according to the combined evaluation criteria (see criteria in section 5).  
 1375

Formula	$r$ (0.5-2) <sup>a</sup> (%)	Formula	$r$ (0.2-5) <sup>b</sup> (%)	Formula	$r$ (0.1-10) <sup>c</sup> (%)	Formula	$mr^d$ (-)	Formula	$m_l r$ (-)	Formula	$gr$ (-)	Formula	$gwr$ (-)
<b>P-K-M</b> <sup>e</sup>	50	<b>B</b>	83	<b>B</b>	97	A-W	1.7	<b>P-K-M</b>	-0.04	<b>B</b>	2.4	<b>P-K-M</b>	2.60
<b>B</b>	47	<b>Y</b>	83	<b>P-K-M</b>	92	<b>P-K-M</b>	2.6	<b>B</b>	-0.09	<b>Y</b>	2.7	<b>R</b>	2.75
<b>Y</b>	44	<b>P-K-M</b>	78	<b>Y</b>	89	<b>B</b>	2.9	<b>R</b>	0.21	<b>P-K-M</b>	2.8	S	2.77
A-W	36	S	75	<b>R</b>	89	<b>R</b>	4.0	<b>Y</b>	0.30	S	3.7	<b>Y</b>	2.79
<b>R</b>	28	<b>R</b>	67	S	86	<b>Y</b>	7.1	A-W	-0.34	<b>R</b>	3.8	A-W	3.70
S	25	A-W	67	Bt	74	Bt	8.4	Bt	0.42	A-W	5.0	<b>B</b>	4.60
Bt <sup>e</sup>	9	Bt	30	A-W	72	S	20.2	S	0.52	Bt	6.9	W-P	10.39
W-P	0	W-P	14	W-P	28	W-P	98.7	W-P	1.27	W-P	18.7	E-B	12.59
E-B	0	E-B	8	E-B	28	E-B	152.5	E-B	1.34	E-B	21.7	Bt	28.16
MP-M	0	MP-M	3	MP-M	11	MP-M	237.3	MP-M	1.62	MP-M	41.9	MP-M	29.06
Eq. (5) <sup>f</sup>	53	Eq. (5)	86	Eq. (5)	94	Eq. (5)	6.5	Eq. (5)	0.20	Eq. (5)	2.5	Eq. (5)	2.95

1376 <sup>a</sup>  $0.5 < r < 2$ , the average percentage of predicted bed load discharge not exceeding a factor of 2 in relation to the observed discharge.  
 1377 <sup>b</sup>  $0.2 < r < 5$ , the average percentage of predicted bed load discharge not exceeding a factor of 5 in relation to the observed discharge.  
 1378 <sup>c</sup>  $0.1 < r < 10$ , the average percentage of predicted bed load discharge not exceeding a factor of 10 in relation to the observed discharge.  
 1379 <sup>d</sup> The values were ranked according to their proximity to  $mr = 1$ . Only for this purpose, the values in the range (0, 1) were recalculated  
 1380 as  $1/mr$ .  
 1381 <sup>e</sup> Formula that directly specify the (surface and/or subsurface) material required to predict bed load discharge. Only values for whose  
 1382 formulae predicted broken armor condition were included (i.e.,  $N = 36$  in case of P-K-M, and  $N = 23$  in Bt). See section 4.3 for more  
 1383 details.  
 1384 <sup>f</sup> Eq. 5 was not included in the formulae performance ranking, it is just presented as a reference.

1386 Table 6. Comparison of the predictive power of the formulae according to the Bed Material Division (BMD) and using the surface bed  
 1387 material to feed the formulae. Note that results are sorted from best to worst performance according to each index. In bold the formulae  
 1388 ranked in the first three positions according to the combined evaluation criteria (see criteria in section 5).  
 1389

Formula	$r$ (0.5-2) <sup>a</sup> (%)	Formula	$r$ (0.2-5) <sup>b</sup> (%)	Formula	$r$ (0.1-10) <sup>c</sup> (%)	Formula	$mr$ <sup>d</sup> (-)	Formula	$m/r$ (-)	Formula	$gr$ (-)	Formula	$gwr$ (-)
<b>P-K-M</b> <sup>e</sup>	50	<b>P-K-M</b>	78	<b>P-K-M</b>	92	<b>P-K-M</b>	2.60	<b>P-K-M</b>	-0.04	<b>P-K-M</b>	2.8	<b>P-K-M</b>	3
<b>Y</b>	28	<b>Y</b>	64	<b>E-B</b>	78	<b>Y</b>	2.80	<b>E-B</b>	0.17	<b>E-B</b>	6.1	<b>Y</b>	6
R	19	<b>E-B</b>	42	Bt	74	W-P	2.90	<b>Y</b>	-0.22	<b>Y</b>	6.5	<b>E-B</b>	10
S	14	R	39	<b>Y</b>	69	R	0.31	Bt	0.42	Bt	6.9	Bt	28
A-W	14	Bt	30	W-P	44	<b>E-B</b>	5.70	MP-M	-0.73	R	44.8	R	149
W-P	11	W-P	25	R	42	A-W	0.15	W-P	-1.19	W-P	59.3	MP-M	162
Bt <sup>e</sup>	9	S	19	MP-M	28	S	0.12	R	-1.61	MP-M	61.7	A-W	862
<b>E-B</b>	6	A-W	19	A-W	25	Bt	8.40	A-W	-2.04	A-W	110.1	W-P	3090
MP-M	3	B	14	B	25	MP-M	9.10	B	-2.13	B	135.6	B	4769
B	3	MP-M	11	S	22	B	0.07	S	-2.21	S	161.8	S	6348
Eq. (5) <sup>f</sup>	53	Eq. (5)	86	Eq. (5)	94	Eq. (5)	6.54	Eq. (5)	0.20	Eq. (5)	2.5	Eq. (5)	3

1390 <sup>a</sup>  $0.5 < r < 2$ , the average percentage of predicted bed load discharge not exceeding a factor of 2 in relation to the observed discharge.

1391 <sup>b</sup>  $0.2 < r < 5$ , the average percentage of predicted bed load discharge not exceeding a factor of 5 in relation to the observed discharge.

1392 <sup>c</sup>  $0.1 < r < 10$ , the average percentage of predicted bed load discharge not exceeding a factor of 10 in relation to the observed discharge.

1393 <sup>d</sup> The values were ranked according to their proximity to  $mr = 1$ . Only for this purpose, the values in the range (0, 1) were recalculated  
 1394 as  $1/mr$ .

1395 <sup>e</sup> Formula that directly specify the (surface and/or subsurface) material required to predict bed load discharge. Only values for whose  
 1396 formulae predicted broken armor condition were included (i.e.,  $N = 36$  in case of P-K-M, and  $N = 23$  in Bt). See section 4.3 for more  
 1397 details.

1398 <sup>f</sup> Eq. 5 was not included in the formulae performance ranking, it is just presented as a reference.

1399

1400 Table 7. Comparison of the predictive power of the formulae according to the Armor Layer Division (ALD). Note that results are sorted  
 1401 from best to worst performance according to each index. In bold the formulae ranked in the first two positions according to the  
 1402 combined evaluation criteria (see criteria in section 5).  
 1403

Formula	$r$ (0.5-2) <sup>a</sup> (%)	Formula	$r$ (0.2-5) <sup>b</sup> (%)	Formula	$r$ (0.1-10) <sup>c</sup> (%)	Formula	$mr^d$ (-)	Formula	$mlr$ (-)	Formula	$gr$ (-)	Formula	$gwr$ (-)
<b>P-K-M<sup>e</sup></b>	47	<b>P-K-M</b>	67	<b>P-K-M</b>	93	<b>P-K-M</b>	0.90	MP-M	-0.01	<b>P-K-M</b>	3.1	<b>Y</b>	2.5
<b>Y</b>	34	<b>Y</b>	66	<b>Y</b>	78	R	0.50	<b>Y</b>	0.17	<b>Y</b>	5.7	E-B	3.0
W-P	24	E-B	54	E-B	76	W-P	2.96	<b>P-K-M</b>	-0.33	E-B	7.5	<b>P-K-M</b>	6.6
S	20	R	51	W-P	71	S	0.27	W-P	-0.68	Bt	12.2	MP-M	7.9
A-W	20	W-P	44	R	61	A-W	0.24	E-B	0.87	MP-M	16.2	W-P	8.9
E-B	17	S	39	MP-M	56	B	0.11	Bt	-1.09	W-P	18.4	R	10.2
R	17	MP-M	32	S	51	MP-M	9.21	R	-1.25	R	21.1	S	24.1
MP-M	10	A-W	32	A-W	44	Bt	0.09	S	-1.86	B	71.8	B	57.3
B	5	B	20	B	42	E-B	100.80	B	-1.86	S	75.0	A-W	63.9
Bt <sup>e</sup>	0	Bt	0	Bt	25	<b>Y</b>	209.30	A-W	-2.09	A-W	126.9	Bt	> 10 <sup>6</sup>
Eq. (5) <sup>f</sup>	41	Eq. (5)	76	Eq. (5)	85	Eq. (5)	388.90	Eq. (5)	0.50	Eq. (5)	5.3	Eq. (5)	2.8

1404  
 1405 <sup>a</sup>  $0.5 < r < 2$ , the average percentage of predicted bed load discharge not exceeding a factor of 2 in relation to the observed discharge.  
 1406 <sup>b</sup>  $0.2 < r < 5$ , the average percentage of predicted bed load discharge not exceeding a factor of 5 in relation to the observed discharge.  
 1407 <sup>c</sup>  $0.1 < r < 10$ , the average percentage of predicted bed load discharge not exceeding a factor of 10 in relation to the observed discharge.  
 1408 <sup>d</sup> The values were ranked according to their proximity to  $mr = 1$ . Only for this purpose, the values in the range (0, 1) were recalculated  
 1409 as  $1/mr$ .  
 1410 <sup>e</sup> Formula that directly specify the (surface and/or subsurface) material required to predict bed load discharge. Only data for the BAL  
 1411 subset were included (i.e.,  $N = 15$  in case of P-K-M, and  $N = 4$  in Bt). See section 4.3 for more details.  
 1412 <sup>f</sup> Eq. 5 was not included in the formulae performance ranking, it is just presented as a reference.

1413



1414 Table 8. Performance of the formulae compared with a selection of recent studies in gravel bed streams

Reference	$N^a$	$r$ (0.5-2) <sup>b</sup> (%)	$r$ (0.2-5) <sup>c</sup> (%)	$r$ (0.1-10) <sup>d</sup> (%)	Observations
Habersack and Laronne (2002)	13	36	-	-	Alpine gravel bed river.
Martin (2003)	4	19	44	75	Annual gravel transport in 10 reaches of a gravel bed river.
Martin and Ham (2005)	3	11	25	47	Average annual gravel transport in 13 reaches of a gravel bed river.
Duan et al. (2006)	3	-	-	57	Low flow in two reaches of a desert gravel bed stream.
Recking (2010)	4	13	27	34	6319 data from 84 reaches of sand and gravel bed rivers.
This study (River Ebro)	10	19	41	57	Regulated river experiencing cycles of armoring.

1415

1416 <sup>a</sup> Number of formulas involved in the study.

1417 <sup>a</sup>  $0.5 < r < 2$ , the average percentage of predicted bed load discharge not exceeding a factor of 2 in relation to the observed discharge.

1418 <sup>b</sup>  $0.2 < r < 5$ , the average percentage of predicted bed load discharge not exceeding a factor of 5 in relation to the observed discharge.

1419 <sup>c</sup>  $0.1 < r < 10$ , the average percentage of predicted bed load discharge not exceeding a factor of 10 in relation to the observed discharge.